Measurements of the Spin and Parity Properties of the Higgs Boson Using the ATLAS Detector

Andrew S. Hard

University of Wisconsin Madison

On behalf of the ATLAS Collaboration

HEP 2013, Valparaiso, Chile
December 19, 2013

Discovered a boson, must establish spin and parity (J^P) quantum numbers

Test alternative J^P against the SM (0^+) and observe which the data favors

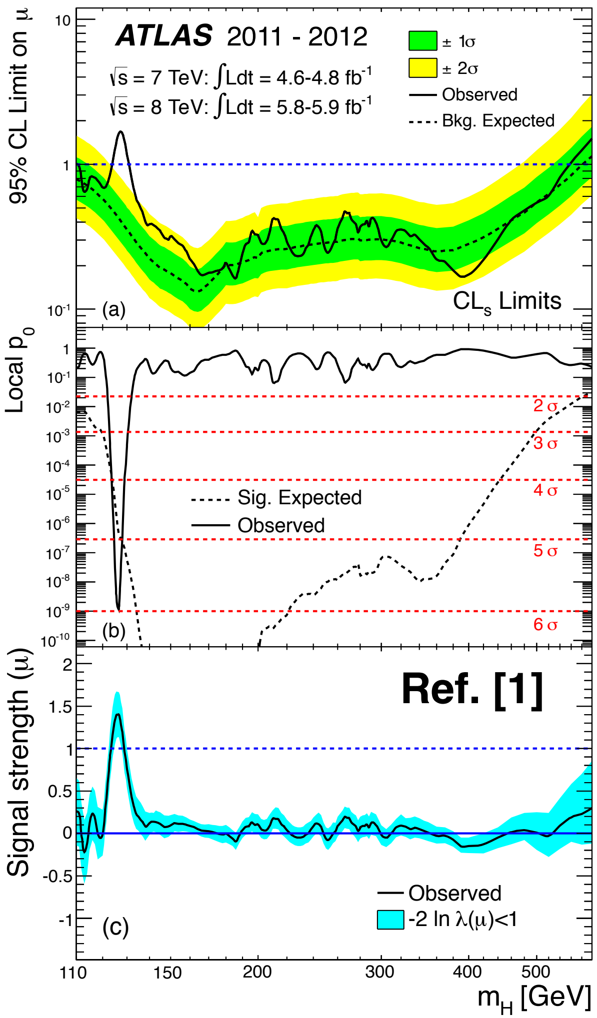

Several alternative models:

- Appearance of boson in **di-photon channel strongly disfavors spin 1** according to Landau-Yang. Can test in $WW^{(*)}$ and $ZZ^{(*)}$ anyway

J^P=2^+

- **Graviton-like tensor**
- minimal couplings to SM particles
- Test production via combinations of *gg* fusion and *qq* annihilation
(beyond the minimal coupling model, which gives 96% gg, 4% qq at LO)

***J*=1 models have signal produced via *qq* annihilation (*gg* forbidden by Landau Yang)**

J^P=0^- models from *gg* production (*qq* negligible)

Bosonic decay channels

Find observables in bosonic channels sensitive to spin and parity that also preserve background discrimination

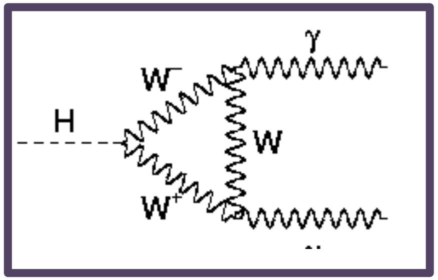

γγ:

- $J^P=0^+$ tested against $J^P= 2^+$ (no parity sensitivity)
- Fit to **the invariant di-photon mass** and **di-photon separation angle**

WW$^{(*)}$→eνμν:

- $J^P=0^+$ tested against $J^P= 1^+, 1^-, 2^+$
- Fit to **multivariate discriminant** from boosted decision trees trained on **4 parameters**

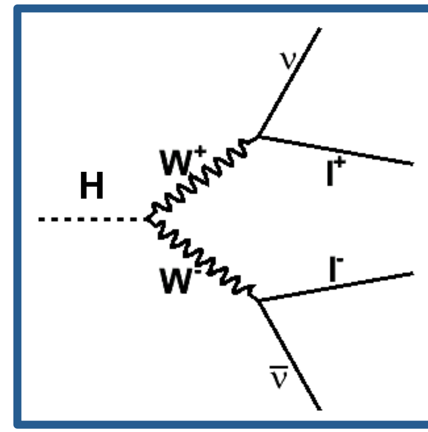

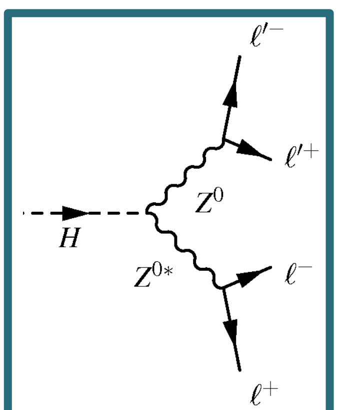

ZZ$^{(*)}$→$l^+l^-l^+l^-$:

- $J^P=0^+$ tested against $J^P= 0^-, 1^+, 1^-, 2^+$
- Fit to **BDT discriminants** trained on **2 mass values, 2 production angles, 3 decay angles**

Signal model from MC

Standard Model Higgs ($J^P=0^+$)

- $ZZ^{(*)}$ channel uses JHU MC generator
- **NLO predictions** from POWHEG MC for $WW^{(*)}$ and $\gamma\gamma$ channels
- Tuned to reproduce the re-summed p_T calculation of the HqT program
- Interfaced with PYTHIA8 for parton showering and hadronization

Alternate spin models (J_{Alt}^P)

- **LO QCD predictions** from JHU generator + PYTHIA8 parton showering
- Transverse momentum comes from parton showering in the initial state
- **p_T of resonance impacts angular variables**
- For gg production, reweight p_T spectrum to POWHEG prediction:

$$w(p_T) = \frac{1}{\sigma_{POWHEG}} \frac{d\sigma_{POWHEG}}{dp_T} \Big/ \frac{1}{\sigma_{PYTHIA}} \frac{d\sigma_{PYTHIA}}{dp_T}$$

- No p_T re-weighting for the qq initial state (LO model has **very large NLO QCD corrections**)

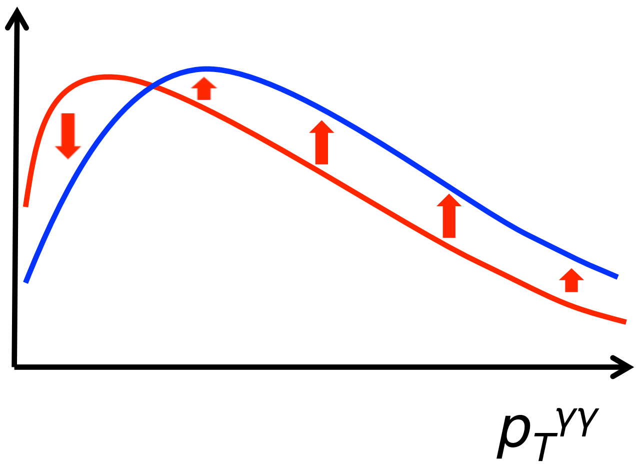

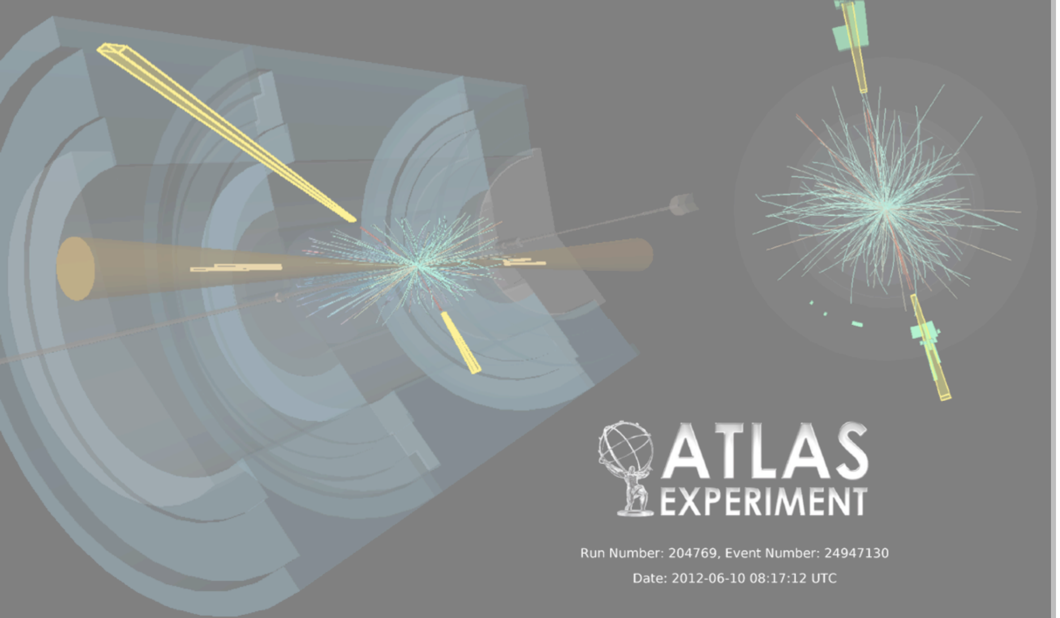

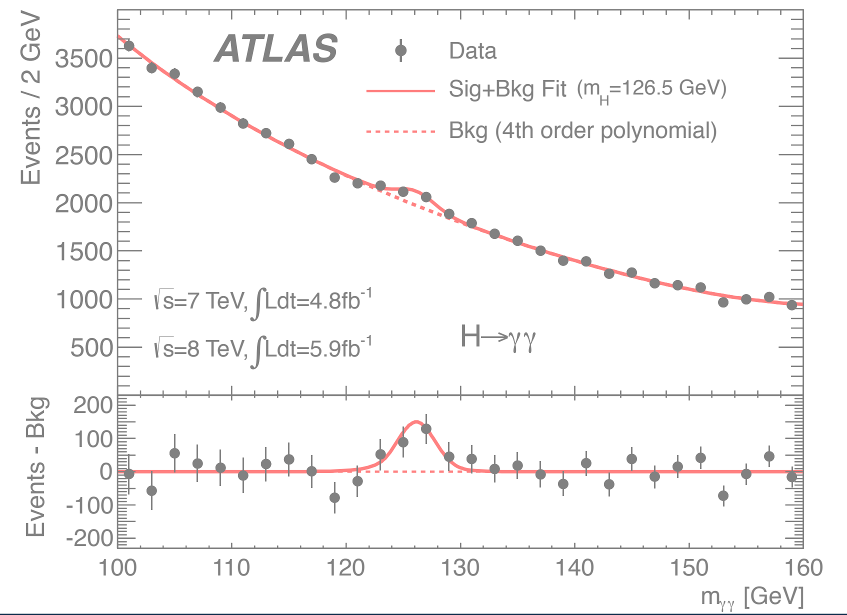

$H\rightarrow\gamma\gamma$ Channel

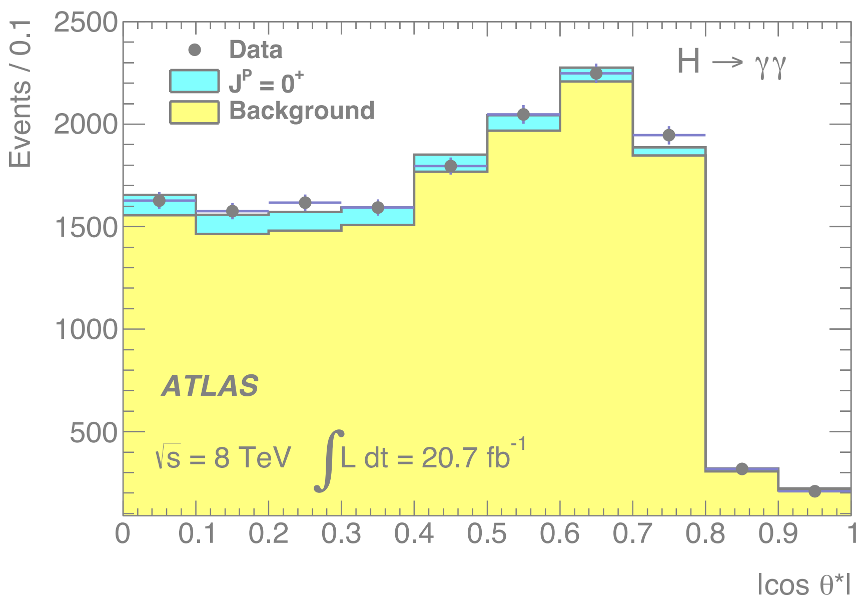

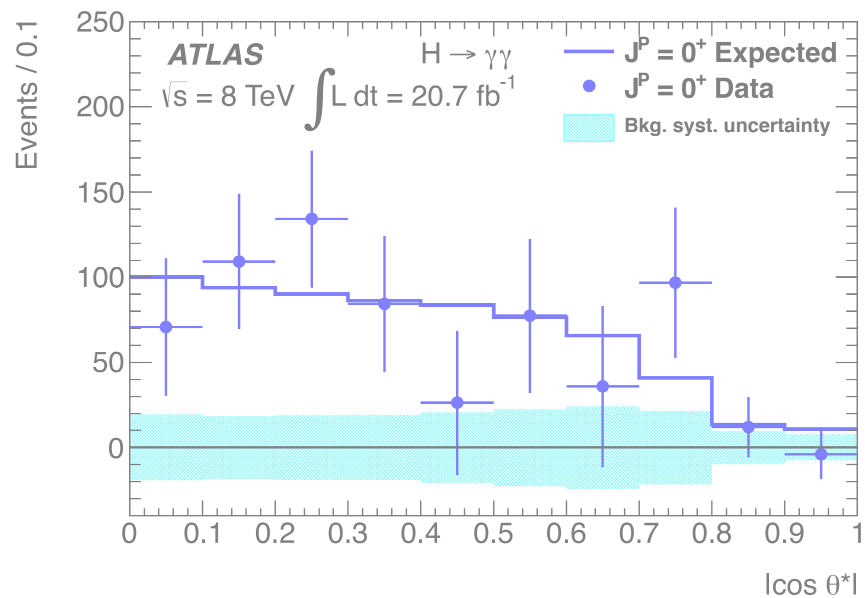

20.7 fb^{-1} of data at $\sqrt{s}$ = 8 *TeV* from the LHC in 2012

Photon selection

- **Energy scale calibration** (and smearing for MC) from $Z \rightarrow ee$
- $p_T > 25$ *GeV*
- $|\eta|<2.37$ excluding $1.37<|\eta|<1.56$ (excluding calo. transition region)
- η corrections from electromagnetic calorimeter pointing.
- Rectangular **"tight" ID cuts** on calorimeter shower shapes.
- **Isolation**:
  ΣE_T^{Calo} (Δr=0.4) < 6.0 *GeV*
  Σp_T^{Track} (Δr=0.2) < 2.6 *GeV*

Event selection

- **Trigger:** "loose" ID di-photon events
- **Vertex reconstruction** with artificial neural network, using pointing capabilities of the ATLAS EM calo. as well as tracking information
- $p_{T,1} / m_{\gamma\gamma} > 0.35$, $p_{T,2} / m_{\gamma\gamma} > 0.25$
- 105 *GeV* $< m_{\gamma\gamma} <$ 160 *GeV*

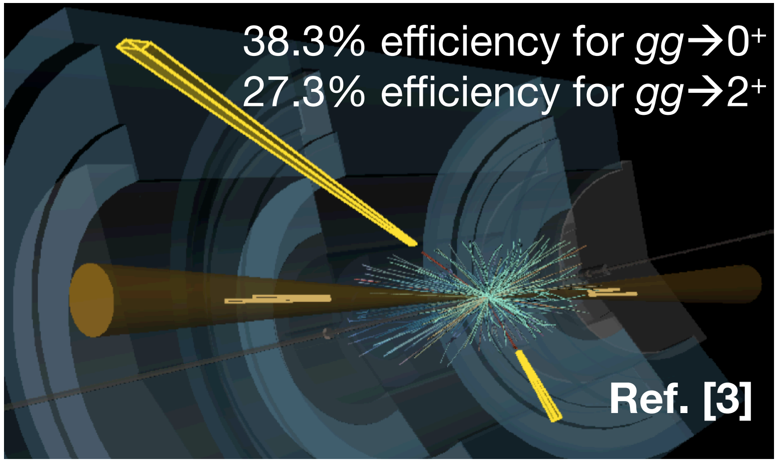

Di-photon invariant mass spectrum

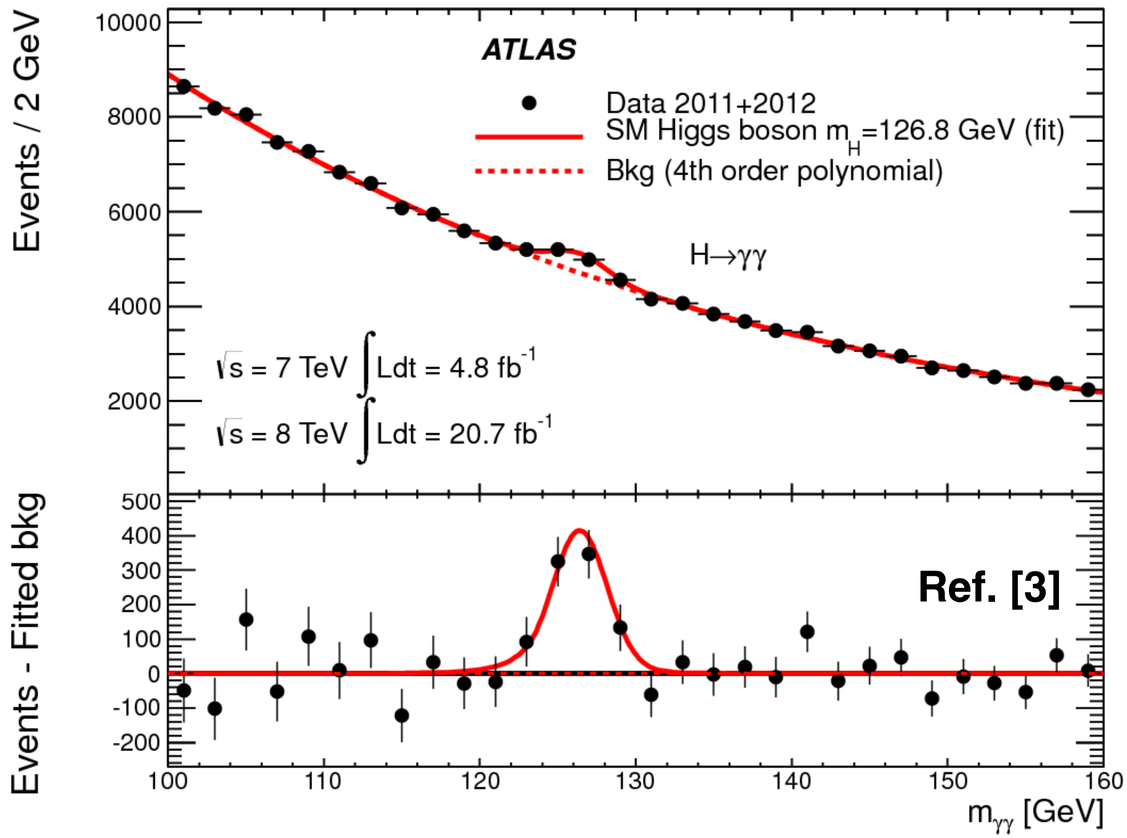

Separate signal from background with fit to the γγ mass

- Excellent **1.77 GeV mass resolution**
- Fit a narrow **signal peak near 125.5 GeV** on top of exponentially decreasing background

Separate 0^+ and 2^+ spin hypotheses using the angular correlation of the two photons

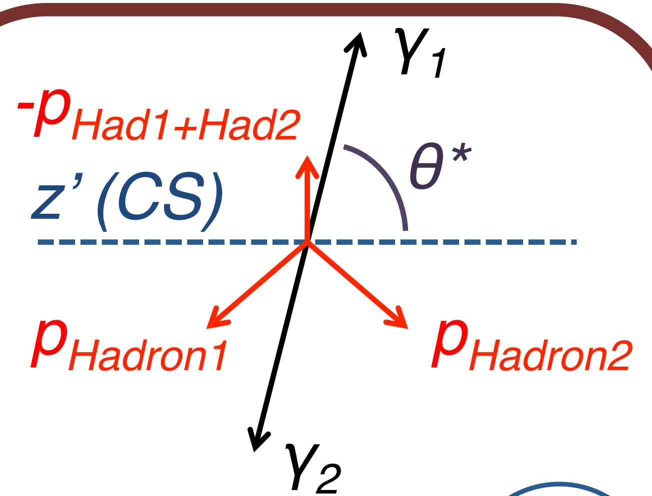

$$\left|\cos\theta^*_{CS}\right| = \frac{\left|\sinh\left(\Delta\eta^{\gamma\gamma}\right)\right|}{\sqrt{1+\left(p_T^{\gamma\gamma}/m_{\gamma\gamma}\right)^2}}\,\frac{2p_T^{\gamma 1}p_T^{\gamma 2}}{m_{\gamma\gamma}^2}$$

Relative p_T cuts on the photons remove most correlation with $m_{\gamma\gamma}$

Collins-Soper frame used to get reference axis z' for $\cos(\theta^*)$

- z-axis bisects angle between the momenta of colliding hadrons
- Minimizes impact of **ISR**
- Better 0^+ / 2^+ discrimination

qq→2^+ very similar to SM *gg*→0^+

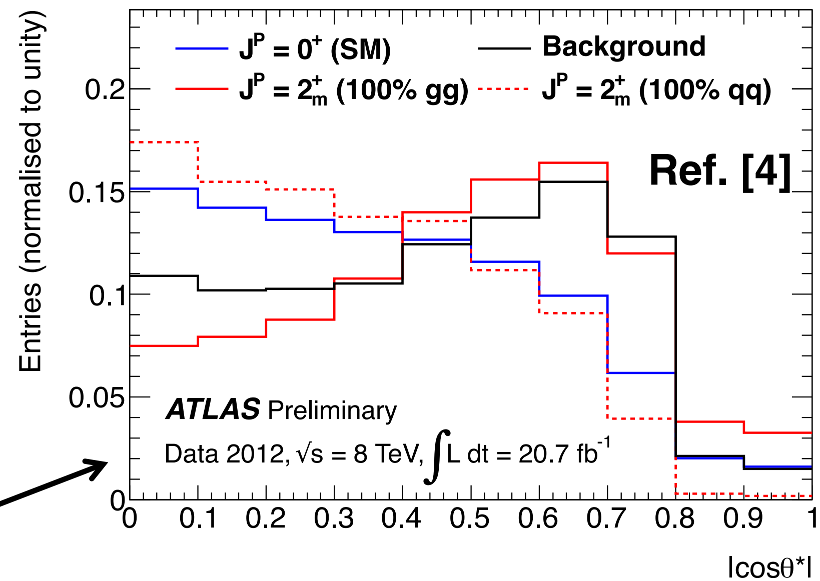

Events are divided into γγ mass sidebands and signal region

Side-bands: 1D fit in $m_{\gamma\gamma}$

- **Background:** O(5) Bernstein polynomial
- Constrains the background shape in the signal region of mass

Signal region: 2D $m_{\gamma\gamma}$-cos(θ*) fit

- Product of two 1D shapes
- **Signal:** Crystal ball + Gaussian mass peak, cos(θ*) shape from MC
- **Background:** cos(θ*) shape from $m_{\gamma\gamma}$ sidebands

Method assumes minimal correlation between mass and cos(θ*) in background

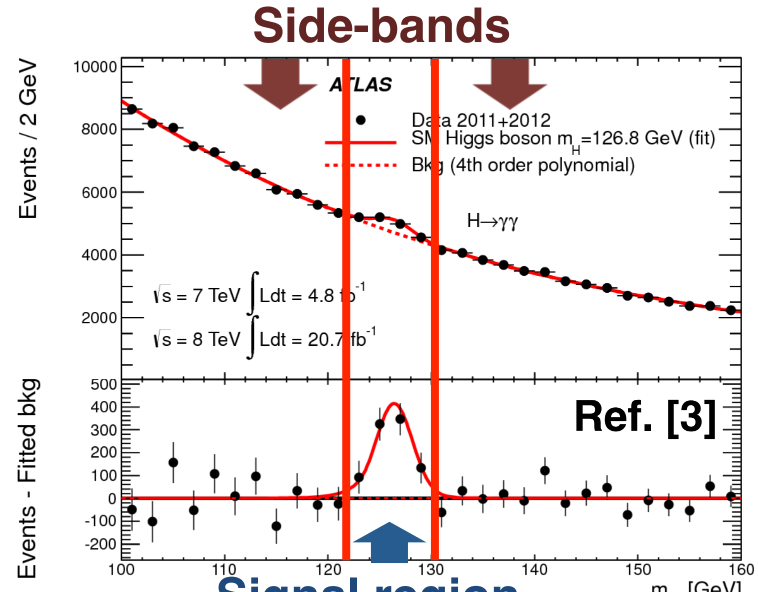

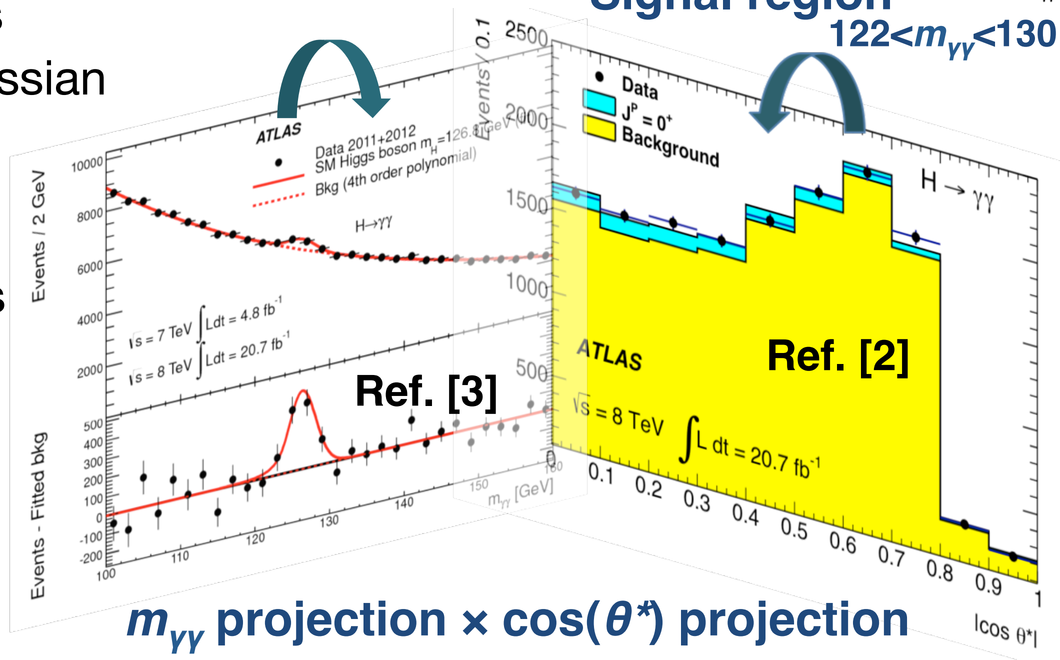

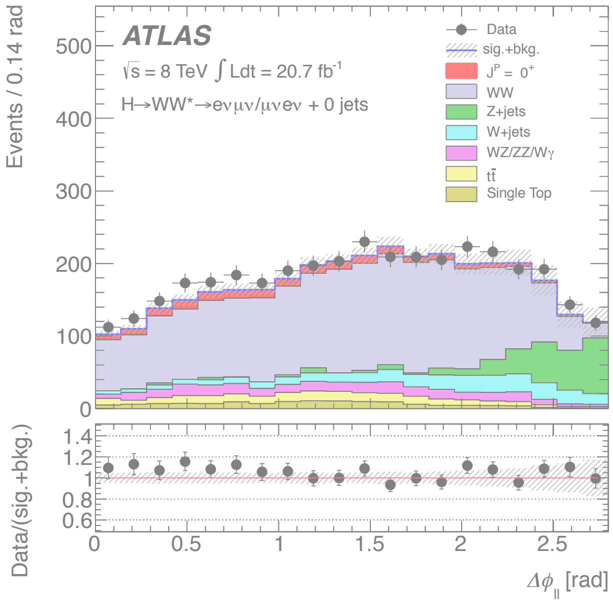

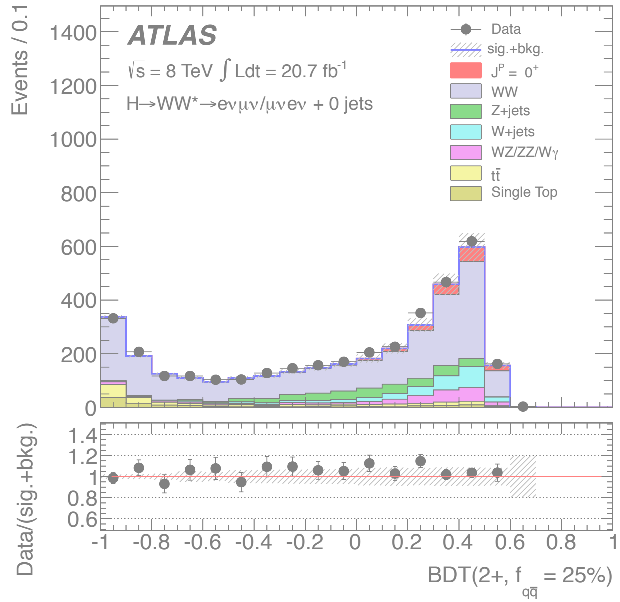

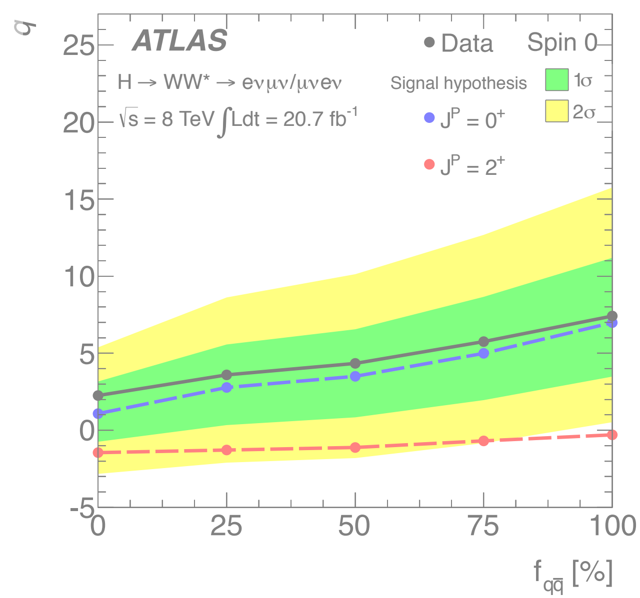

$H \to WW^{(*)} \to e\nu\mu\nu$ Channel

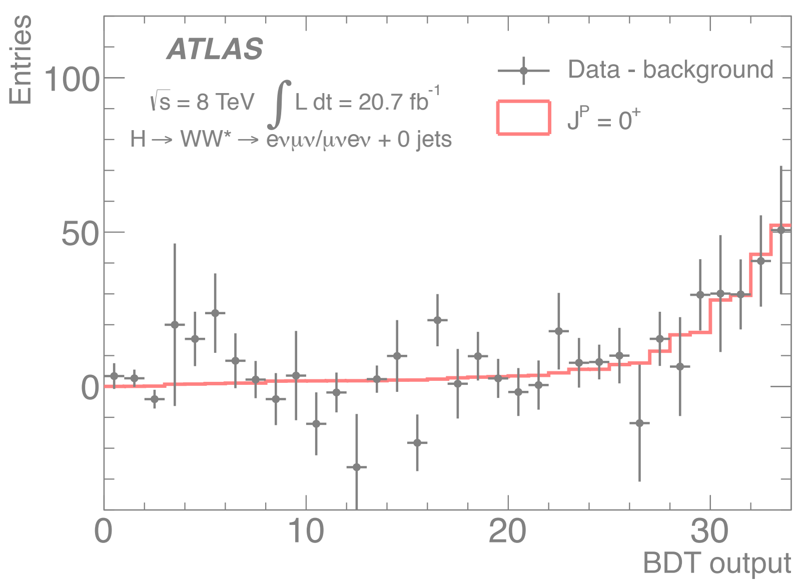

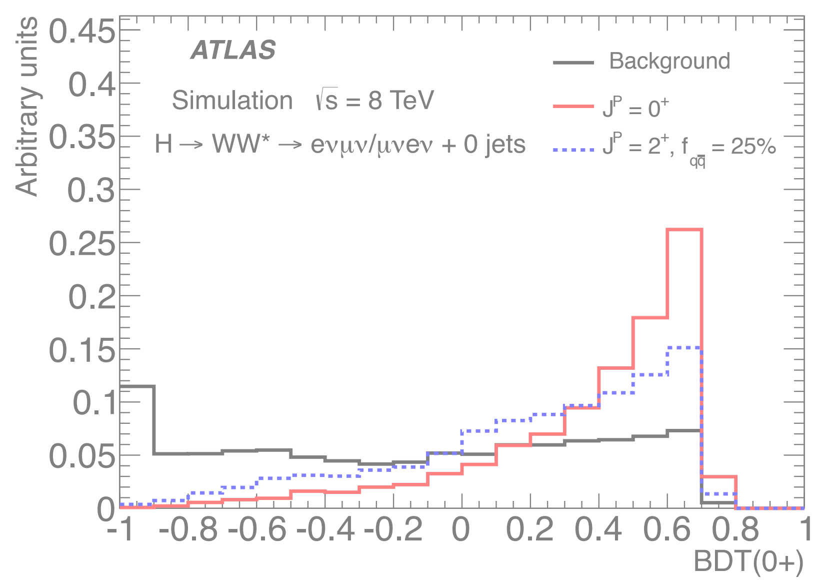

Data sample and event selection

$WW^{(*)} \rightarrow e\nu\mu\nu$ analysis uses full 20.7 fb^{-1} of data at $\sqrt{s}$=8 TeV

- **Trigger** on isolated single-muon and single-electron events with p_T>24 GeV

Lepton selection

- $|\eta^{lepton}| < 2.5$ (inside tracker volume)
- $p_T^{lepton1} > 25$ GeV and $p_T^{lepton2} > 15$ GeV

Event selection

- Veto events with jets
- Require exactly **1 electron** and **1 muon** of opposite charge
- Di-lepton transverse momentum cut (reduce Z+jets): $\boldsymbol{p_T^{ll} > 20}$ **GeV**
- Di-lepton invariant mass: $\boldsymbol{m_{ll} < 80}$ **GeV**
- Azimuthal separation of leptons: $\boldsymbol{\Delta\phi_{ll} < 2.8}$
- $\boldsymbol{MET_{Rel} > 20}$ **GeV**

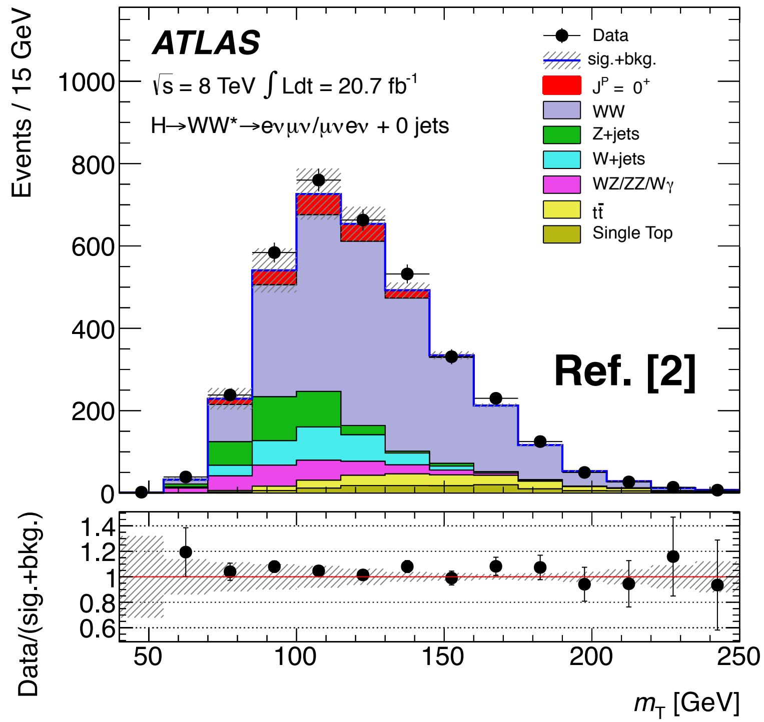

Transverse mass distribution after selection (signal region)

$$MET_{REL} = \begin{cases} E_T^{Miss} & \Delta\phi \geq \frac{\pi}{2} \\ E_T^{Miss} \cdot \sin\Delta\phi & \Delta\phi < \frac{\pi}{2} \end{cases}$$

Estimating the primary backgrounds

MC simulation distributions normalized to observed rates in control regions

WW

- **Control region:** no **$\Delta\phi_{ll}$** cut, **m_{ll}** cut inverted
- Subtract off non-WW contributions (from MC)

Z/γ* + Jets

- **Control region:** invert **$\Delta\phi_{ll}$** cut, remove **p_T^{ll}** cut
- Suppressed in signal region by MET_{Rel} cut

W + hadronic jet mis-tagged as a lepton

- **Control region:** “reversed” lepton selection
- Fully data-driven estimation

Di-boson (WW, WZ/γ*, ZZ/γ*)

- Shapes and normalizations estimated **from MC**, checked in validation regions

Top quark (tt and single top) production

- Estimated in **2 CR**: (1) all events after MET_{Rel} cut (2) events with 1b-jet after MET_{Rel} cut

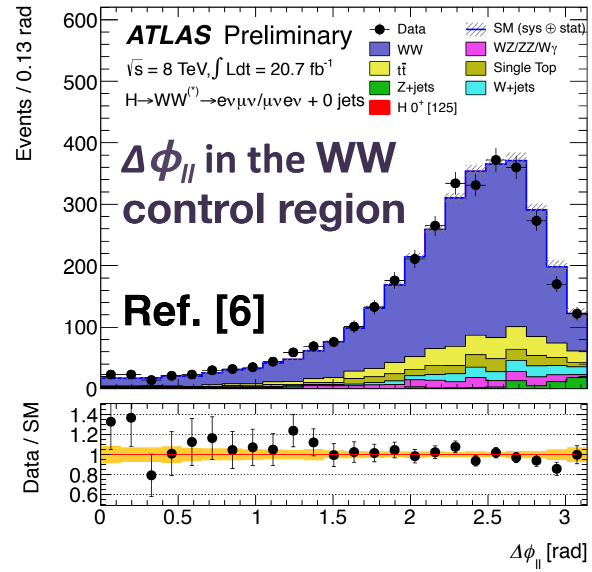

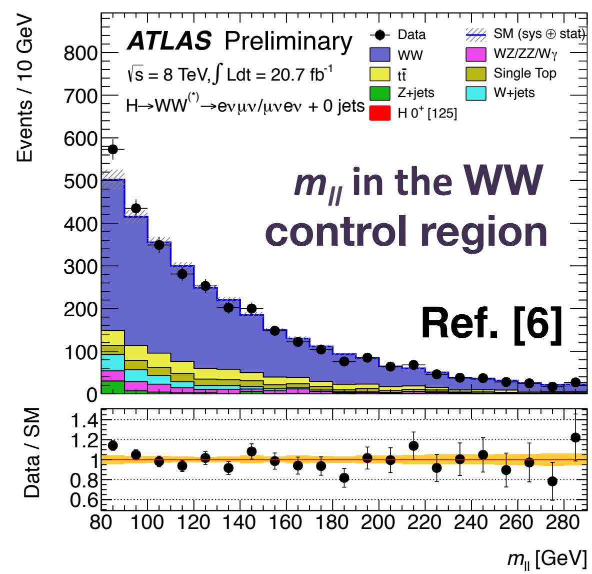

Analysis method

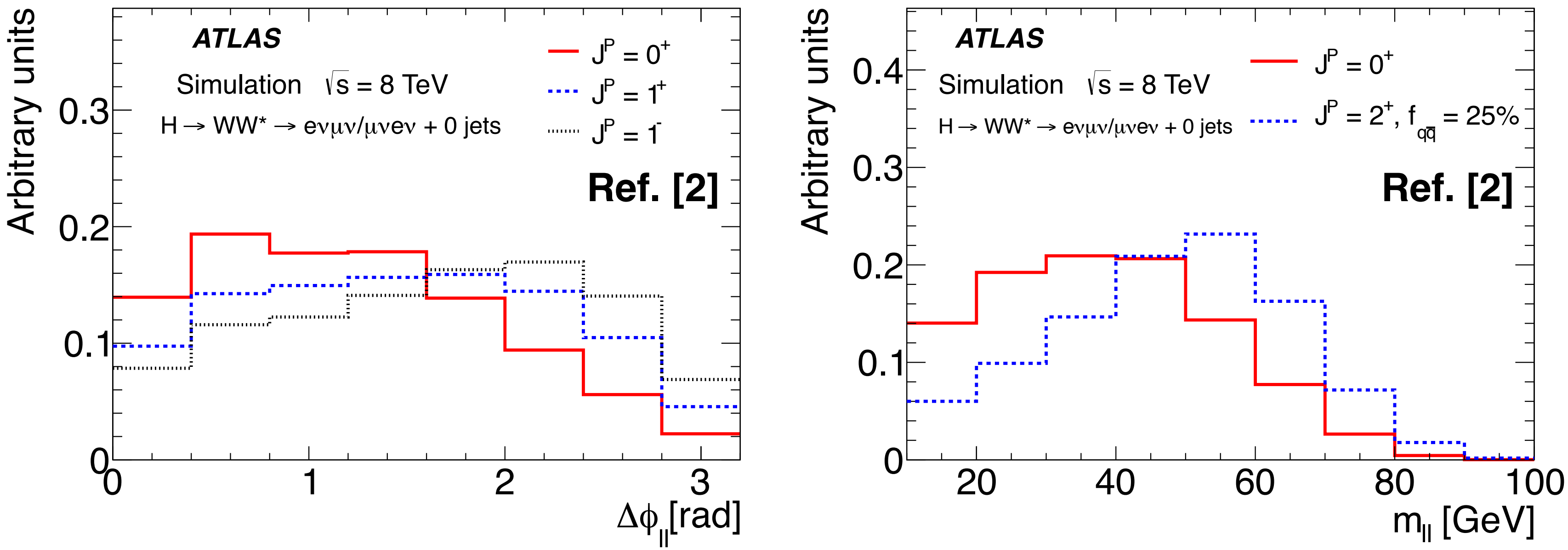

Spin correlations between decay products affect event topologies

- Can't directly calculate angles due to non-interacting neutrinos
- m_{ll} and and $\Delta\phi_{ll}$ are the two variables most sensitive to spin

Use boosted decision trees to perform shape-based analysis

Train 2 BDT classifiers for each hypothesis test: one to distinguish SM J^P=0⁺ from all the backgrounds, one to separate alternative spin hypotheses (J^P=2⁺, 1⁺, 1⁻) from all backgrounds

- **4 variables:** m_{ll}, $\Delta\phi_{ll}$, p_T^{ll}, m_T sensitive to spin, reduce background

2D distributions of BDT classifier outputs used in binned likelihood fits to test compatibility with each J^P hypothesis

- Construct unique 2D BDT distribution for each hypothesis test

Overall, test separation of Standard Model $J^P=0^+$ hypothesis against $J^P=1^+,1^-,2^+$ (no sensitivity to 0^-)

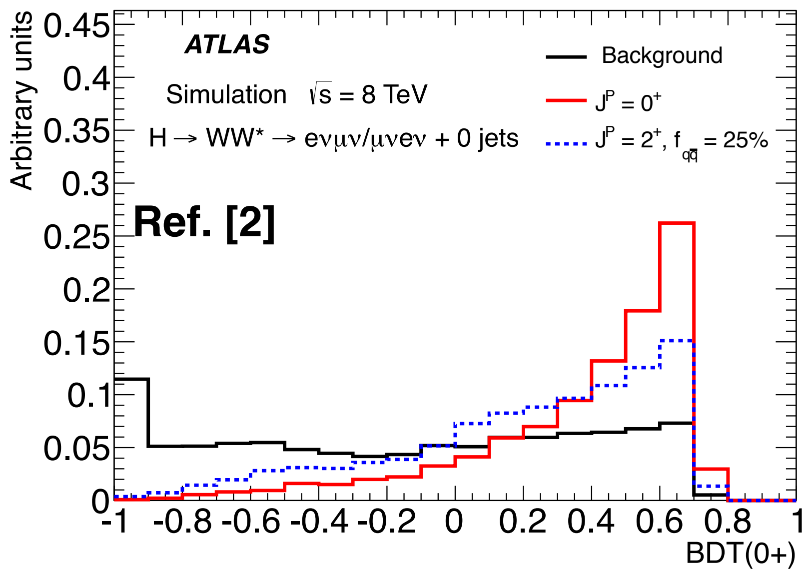

Expected BDT output distributions in the signal region, trained with $J^P=0^+$

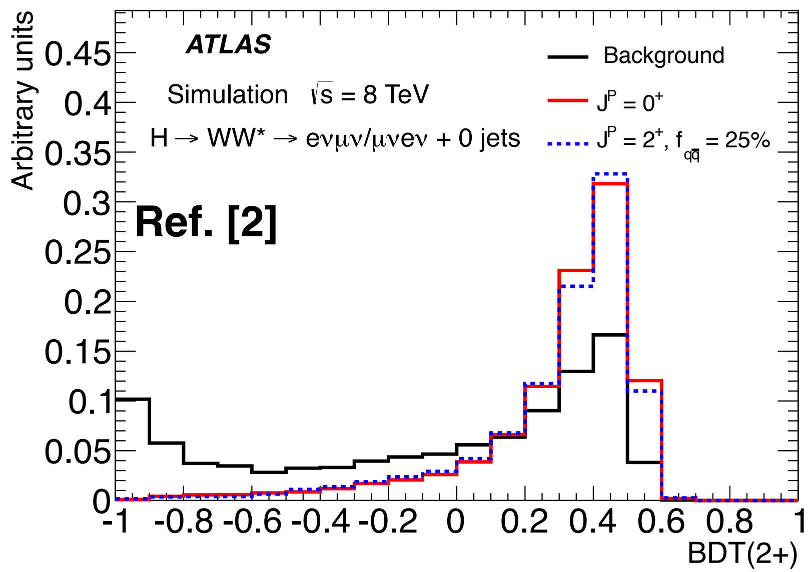

Expected BDT output distributions in the signal region, trained with $J^P=2^+$

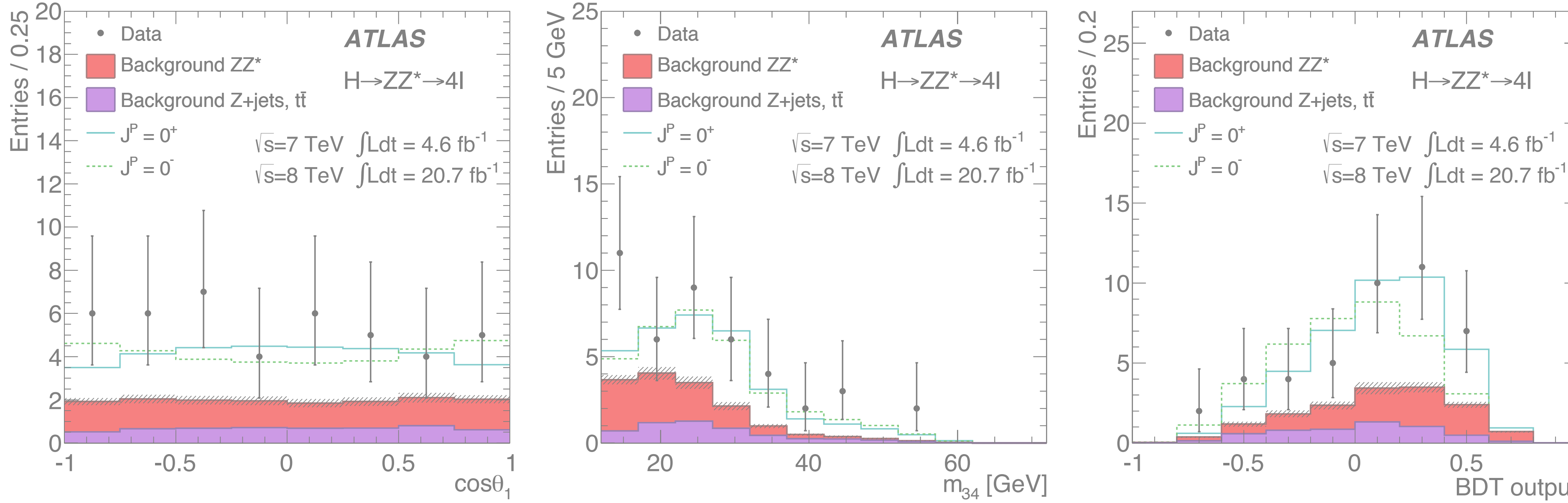

$H \rightarrow ZZ^{(*)} \rightarrow l^+l^-l^+l^-$ Channel

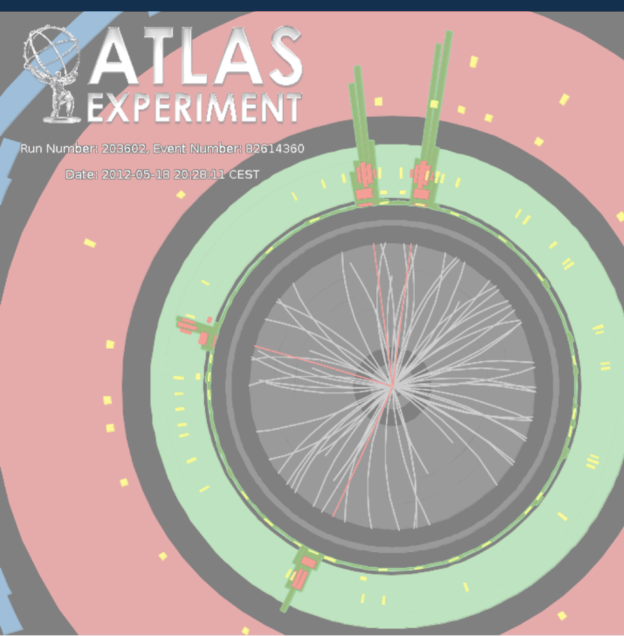

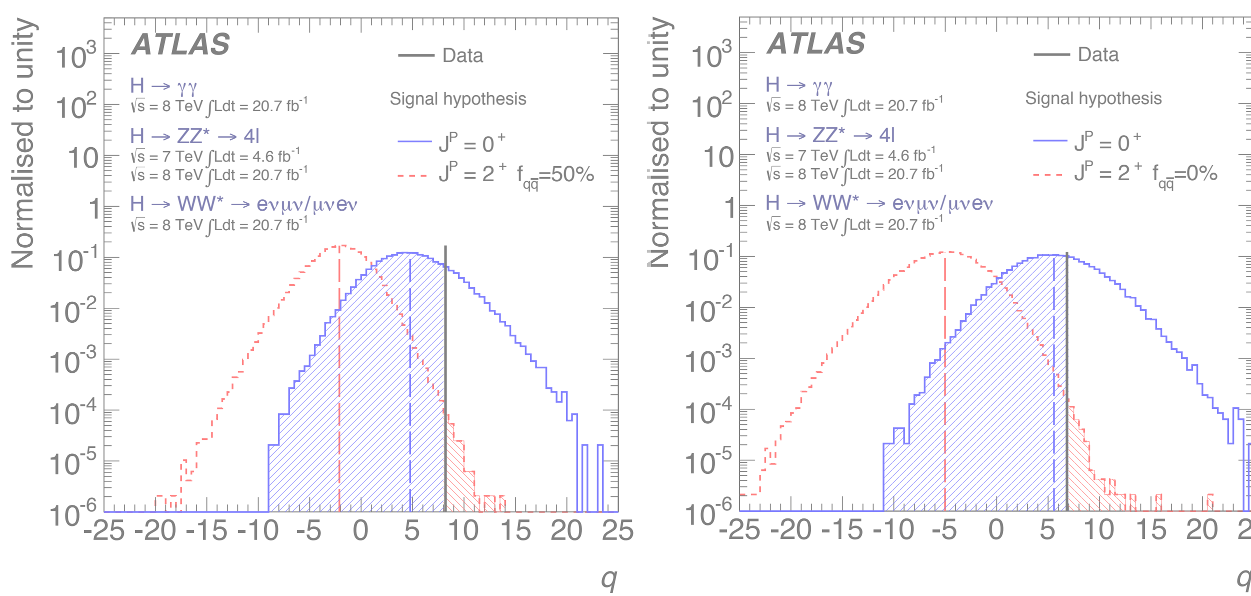

4.6 fb^{-1} of data at $\sqrt{s}$=7 *TeV* and
20.7 fb^{-1} of data at $\sqrt{s}$=8 *TeV*

Trigger: single and di-lepton events

Electron selection

- p_T^{ele} > 7 GeV, $|\eta_{ele}|$ < 2.47
- Optimized multi-lepton identification

Muon selection

- p_T^{μ} > 6 GeV, $|\eta_{\mu}|$ < 2.7
- Muon ID cuts (described in Ref[7])

Lepton isolation & impact parameter cuts

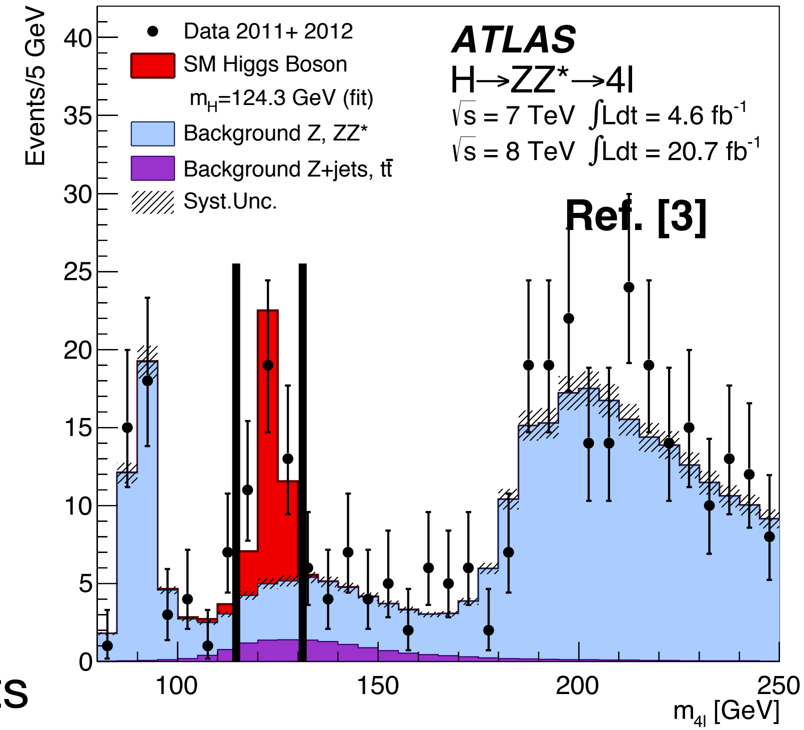

Small branching ratio & large S/B

Event selection

- Tighter cuts on the leading lepton p_T
- Require 2 pairs of **same-flavor opposite-charge leptons**
- Select pair with mass closest to Z mass, require **50 < m_{12} < 106 GeV**
- Events **categorized by flavor of lepton pairs** to increase sensitivity

Study spin-sensitive observables in 115 GeV<m_{4l}<130 GeV window

Background estimation

Non-resonant *ZZ* is the dominant (irreducible) background

- Estimated from MC, normalized to NLO calculations

***Z+jets* and *tt* estimated from data control regions**

- Estimate transfer factor using background-enriched region in MC

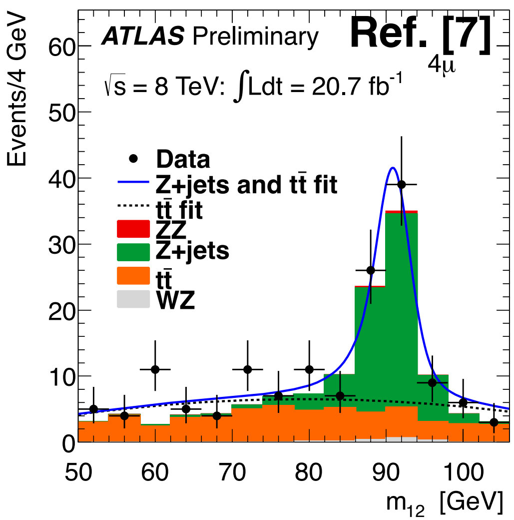

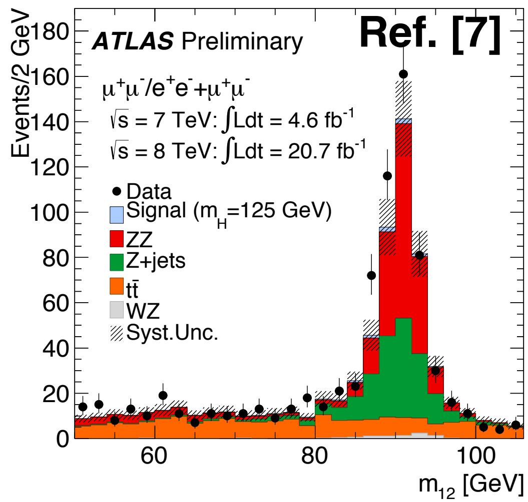

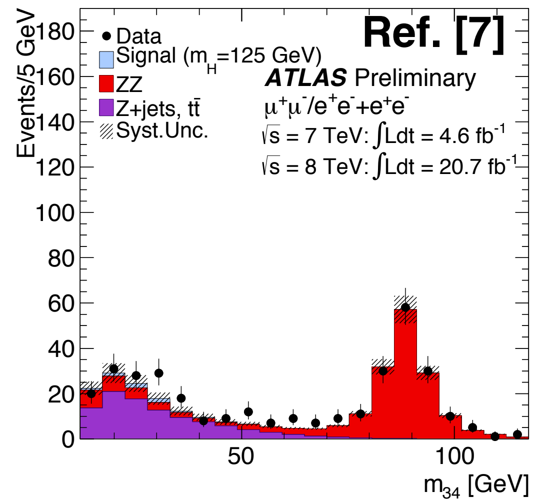

***ll* + $\mu^+\mu^-$ control region**

- Reverse isolation and impact parameter cuts
- Obtain yields of *Z+jets* and *tt* with fit to control region

3 control regions for *ll* + e^+e^-

1. Relax isolation and impact parameter cuts
2. Reverse isolation and impact parameter cuts for one lepton
3. Same-flavor same-sign di-electron pairs

Many observables provided by the fully reconstructed 4 lepton final state

- **Production angles Φ_1, θ^*** and **decay angles θ_1, θ_2, Φ**, illustrated in the figure
- m_{34} and m_{12} play a very important role in discrimination

Combine angles using multivariate discriminant based on a boosted decision tree

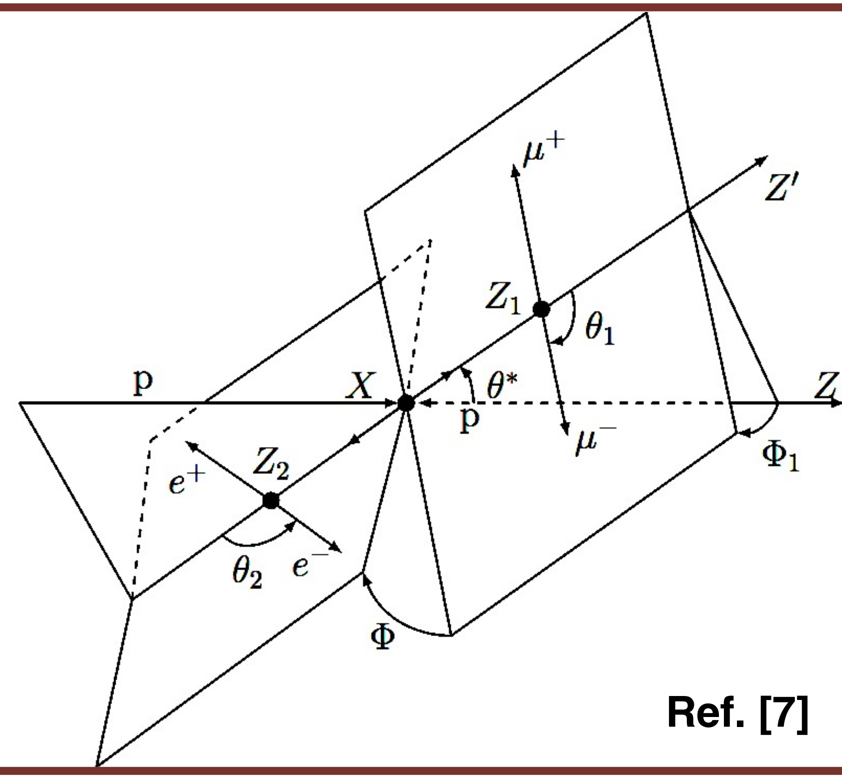

Ref. [7]

Independently train BDT classifiers for each signal hypothesis

- **7 input variables**: 5 production and decay angles as well as masses of the two Z bosons ($\mathbf{m}_{1,2}$ and $\mathbf{m}_{3,4}$)
- Test SM J^P=0^+ as well as J^P=0^-, 1^+, 1^-, 2^+
- For J^P=2^+, train BDTs for different fractions of $qq \rightarrow 2^+$ production

Responses of BDTs evaluated separately for each pair of signal hypotheses

- Perform signal-plus-background fit to the BDT discriminant for each hypothesis

Improve overall sensitivity by evaluating BDT responses in regions with high and low signal/background

- **Low *S/B*:** $115 < m_{4l} < 121$ GeV or $127 < m_{4L} < 130$ GeV
- **High *S/B*:** $121 < m_{4l} < 127$ GeV

Analyses using matrix element-based discriminant give compatible results

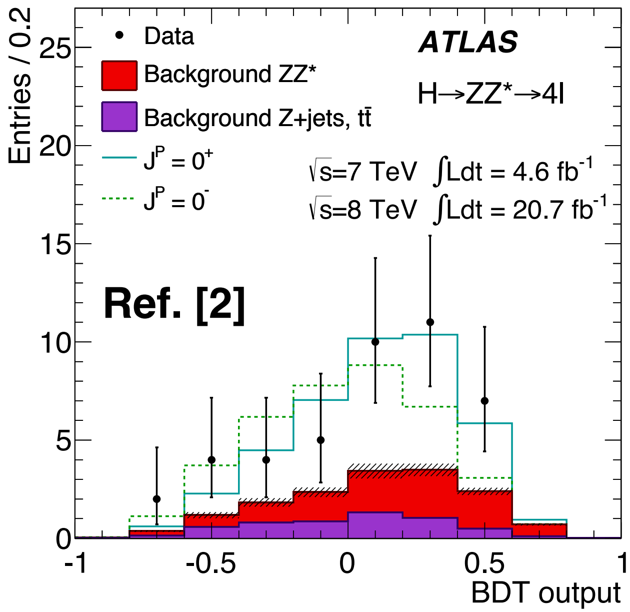

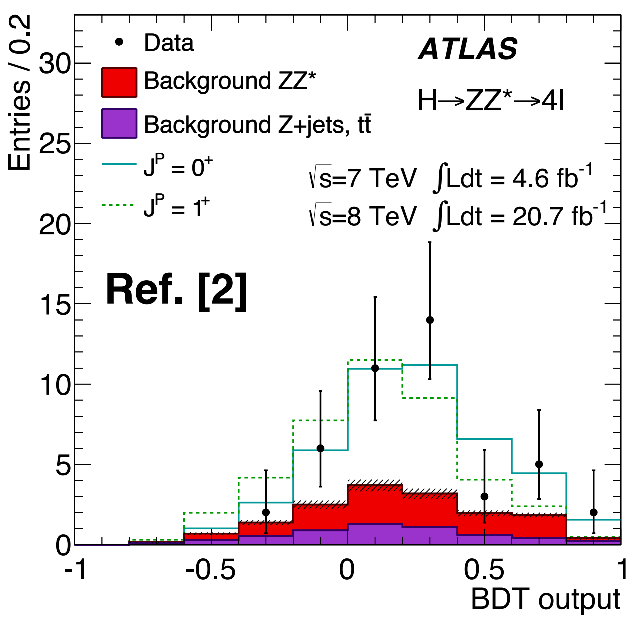

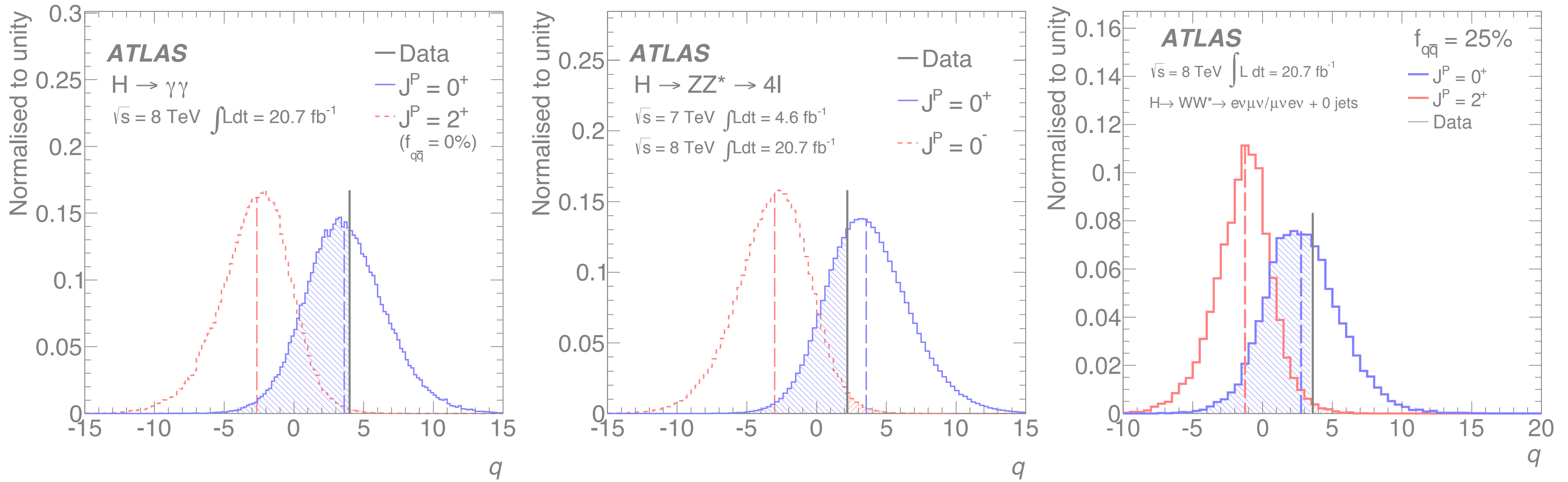

Combination of Channels

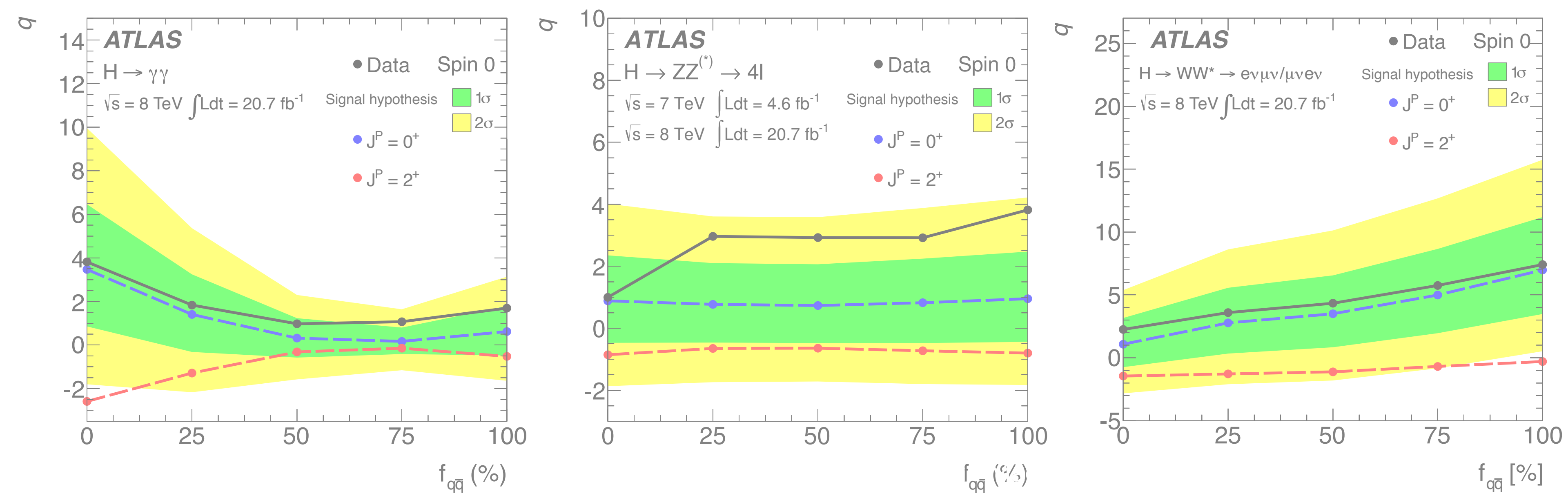

Each channel has observables that discriminate between J^P hypotheses and between signal and background

Construct a likelihood function L that depends on the spin-parity assumption of the signal

- Product of conditional probabilities over binned distributions of the discriminants:

J^P-dependent signal expectation

$$L\left(J^P,\mu,\theta\right)=\prod_{j}^{N_{Channel}}\prod_{i}^{N_{Bins}}\underbrace{P\left(N_{i,j}\middle|\mu_j\cdot S_{i,j}^{J^P}(\theta)+B_{i,j}(\theta)\right)}_{\text{Poisson Component}}\times\underbrace{A_j(\theta)}_{\text{Constraint Component}}$$

Poisson Component

Constraint Component

- **μ** is the **signal rate nuisance parameter** in the channel *j*, and is treated as an unconstrained nuisance parameter
- **θ** represents the **other nuisance parameters**

Statistical test for all channels

Construct a likelihood ratio test-statistic to separate hypotheses

$$q = \log \frac{L\left(J^P = 0^+, \hat{\hat{\mu}}_{0^+}, \hat{\hat{\theta}}_{0^+}\right)}{L\left(J^P_{Alt}, \hat{\hat{\mu}}_{J^P_{Alt}}, \hat{\hat{\theta}}_{J^P_{Alt}}\right)}$$

- $\hat{\hat{\mu}}$ and $\hat{\hat{\theta}}$ represent the fitted signal strength and other nuisance parameters

Get expected distribution of test statistic from unconditional ensemble tests (MC pseudo-experiments)

- Values of nuisance parameters like μ are fixed to those from fit to data

Calculate CL_S from p_0 values from ensemble test statistic distributions

$$CL_S(J^P_{Alt}) = \frac{p_0(J^P_{Alt})}{1 - p_0(0^+)}$$

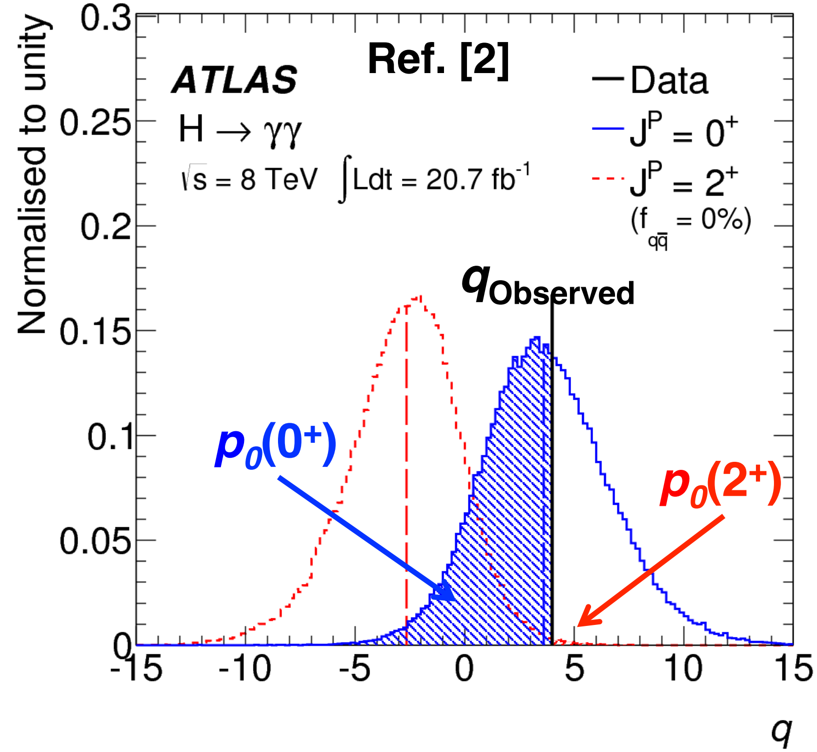

Example distributions of the test statistics $g_{0+}(q)$ and $g_{2+}(q)$ from pseudo-experiments.

Expected and observed values of the test statistic as a function of the $qq \rightarrow 2^+$ production fraction by channel

Sensitivity for the channels is complementary

- $\gamma\gamma$ has better hypothesis discrimination at low f_{qq}
- $ZZ^{(*)}$ sensitivity is stable with respect to f_{qq}
- $WW^{(*)}$ have better discrimination at high f_{qq}

Observations in each channel favor SM J^P=0⁺ over 2⁺

γγ channel

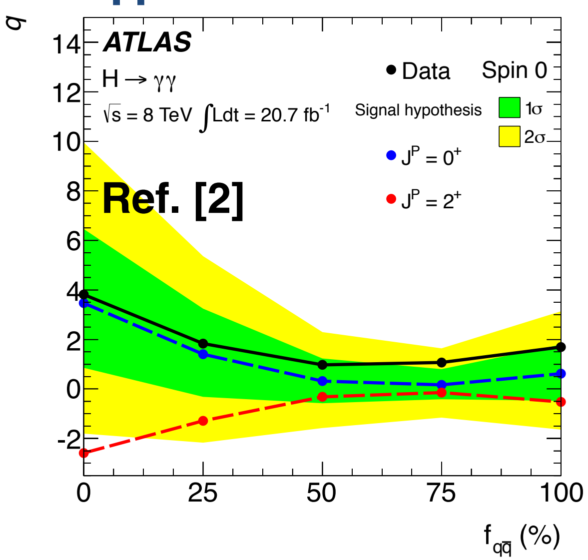

ZZ(*) channel

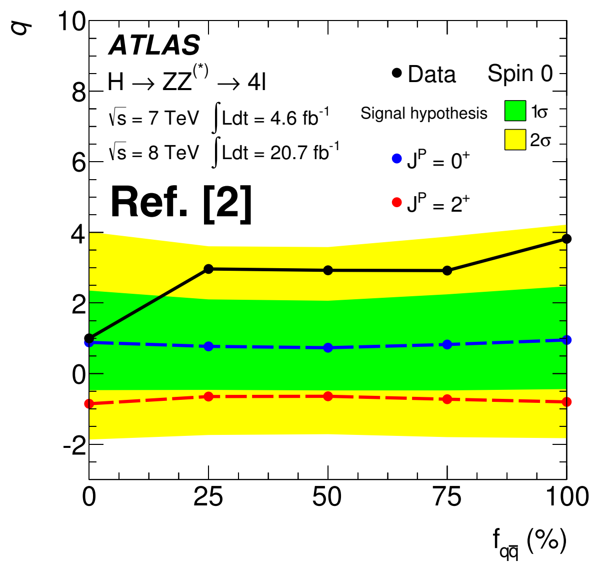

WW(*) channel

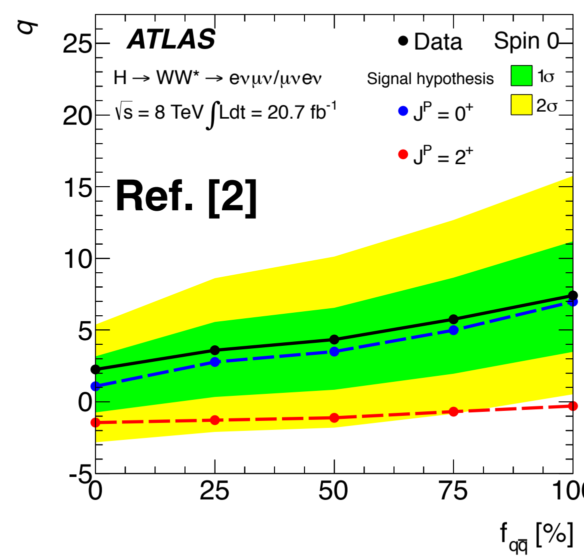

CL_S from the combination of channels

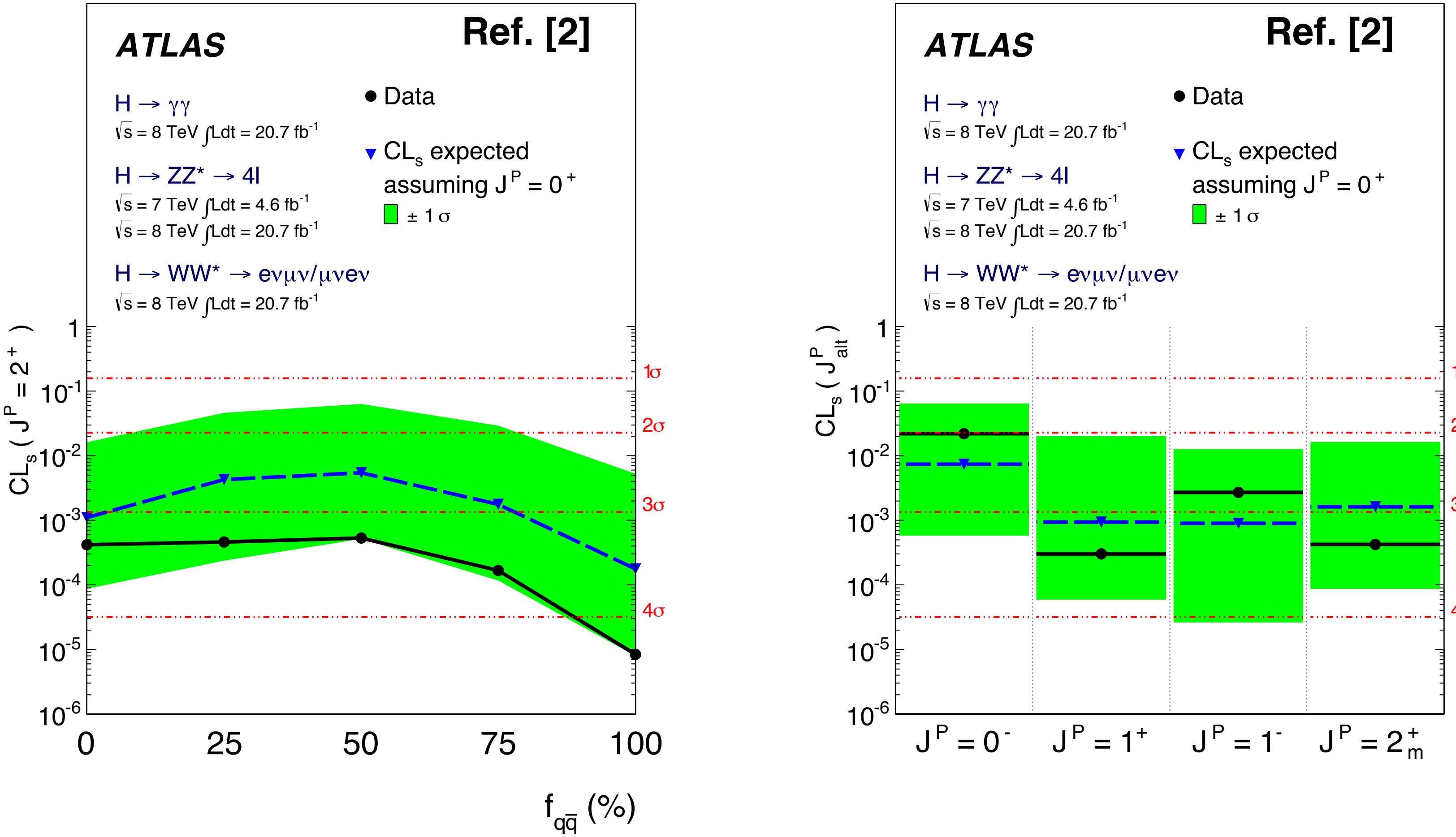

Exclusion of J^P=2⁺ with respect to the Standard Model J^P=0⁺ extends beyond **3σ significance** for all fractions of $qq \rightarrow 2^+$ signal production

In addition, the data clearly **disfavors J^P=0⁻, 1⁺ and 1⁻ hypotheses** in favor of the Standard Model hypothesis

ATLAS has made significant progress in understanding the spin/CP properties of the new boson with the $\gamma\gamma$, $WW^{(*)}$, and $ZZ^{(*)}$ channels

Hypothesis tests on 7 TeV + 8 TeV dataset strongly favor the Standard Model hypothesis ($J^P=0^+$)

- Exclude minimal $J^P=2^+$ models at > 3σ significance
- Other models ($J^P= 0^-, 1^+, 1^-$) disfavored by data

Stay tuned for final 7 TeV + 8 TeV dataset publications!

- Including tests of signals with CP admixture

References

1. *Observation of a new particle in the search for the Standard Model Higgs Boson with the ATLAS detector at the LHC*
   http://www.sciencedirect.com/science/article/pii/S037026931200857X
   auxiliary plots:
   https://atlas.web.cern.ch/Atlas/GROUPS/PHYSICS/PAPERS/HIGG-2012-27/

2. *Evidence for the spin-0 nature of the Higgs boson using ATLAS data*
   http://arxiv.org/abs/1307.1432
   auxiliary plots:
   https://atlas.web.cern.ch/Atlas/GROUPS/PHYSICS/PAPERS/HIGG-2013-01/

3. *Measurement of the Higgs boson production and couplings in diboson final states with the ATLAS detector at the LHC*
   http://arxiv.org/abs/1307.1427
   auxiliary plots:
   https://atlas.web.cern.ch/Atlas/GROUPS/PHYSICS/PAPERS/HIGG-2013-02/

4. *Study of the spin of the Higgs-like boson in the two photon decay channel using 20.7 fb^{-1} of pp collisions collected at $\sqrt{s}$=8 TeV with the ATLAS detector*
   https://cds.cern.ch/record/1527124

5. *Measurements of the properties of the Higgs-like boson in the two photon decay channel with the ATLAS detector using 25 fb^{-1} of proton-proton collision data*
   http://cds.cern.ch/record/1523698

6. *Study of the spin properties of the Higgs-like boson in the $H \rightarrow WW^{(*)} \rightarrow e\nu\mu\nu$ channel with 21 fb^{-1} of $\sqrt{s}$=8 TeV data collected with the ATLAS detector*
   https://cds.cern.ch/record/1527127

7. *Measurements of the properties of the Higgs-like boson in the four lepton decay channel with the ATLAS detector using 25 fb^{-1} of proton-proton collision data*
   http://cds.cern.ch/record/1523699

8. *L. J. Dixon and M. S. Siu, Resonance continuum interference in the diphoton Higgs signal at the LHC*, Phys. Rev. Lett. 90 (2003) 252001, arXiv:hep-ph/ 0302233 [hep-ph]
   http://arxiv.org/pdf/hep-ph/0302233.pdf

Appendix

Experimental systematic uncertainties

γγ channel

- cos(θ*) shape uncertainty from $J^P=2^+$ MC p_T modeling
- Interference with non-resonant $\gamma\gamma$ background
- 2% uncertainty due to residual correlation between $m_{\gamma\gamma}$ and cos(θ*)
- Spurious signal from background model bias

WW channel

- Dominated by jet energy scale and resolution uncertainties
- Lepton energy scales and resolutions
- W+jets background CR→SR transfer factor
- $J^P=2^+$ p_T spectrum shape uncertainty
- Theory shape and normalization uncertainty for WW background

ZZ channel

- Shapes of BDT output, normalizations of different S/B regions due to lepton energy scale and resolution
- ±10% on normalization of high and low S/B mass regions (uncertainty on Higgs boson mass)
- Others related to overall background yields

Combination: test statistic distributions for $J^P=2^+$ tests

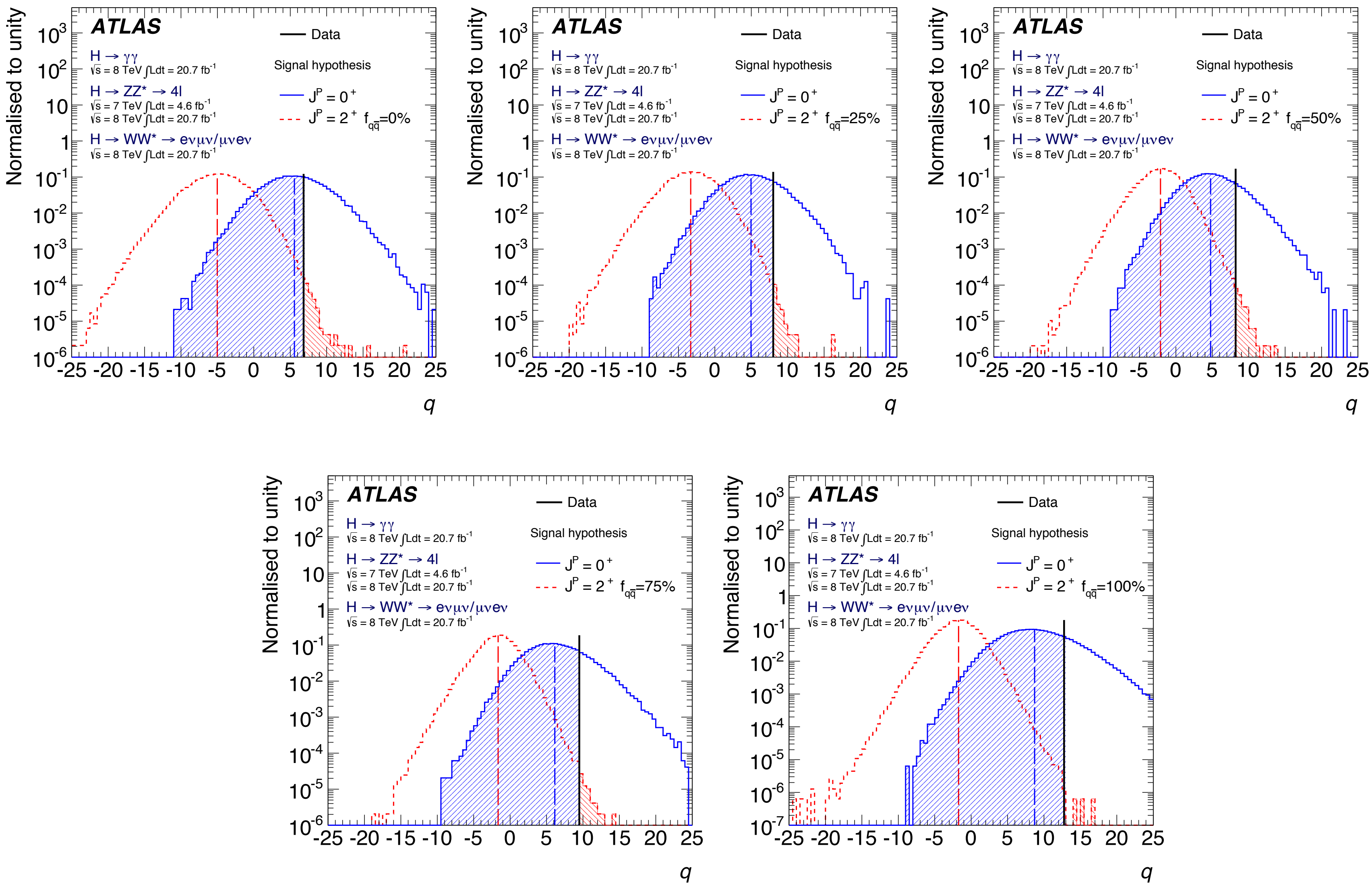

$\gamma\gamma$ channel: background-subtracted cos(θ*) distribution

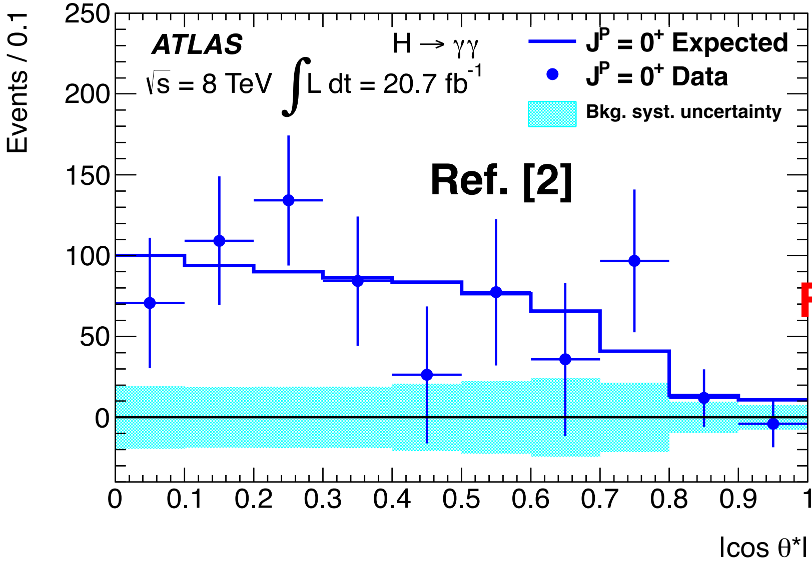

Favored by the data

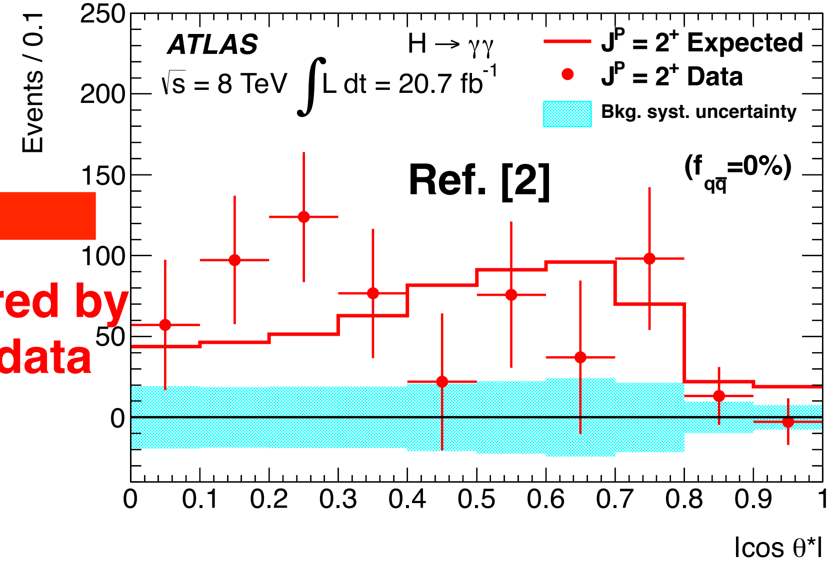

Fit (points) and 0^+ expectation (line)

Fit (points) and *gg*→2^+ expectation (line)

$\gamma\gamma$ channel: correlation between $m_{\gamma\gamma}$ and $\cos(\theta^*)$

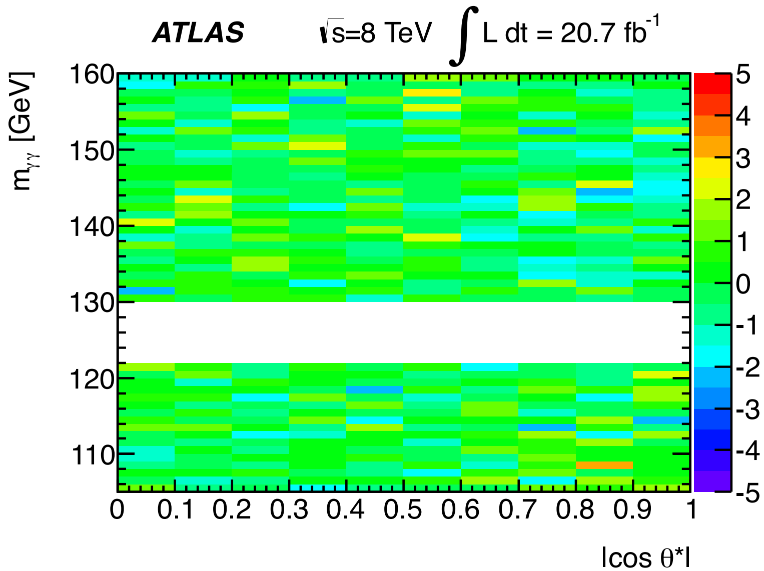

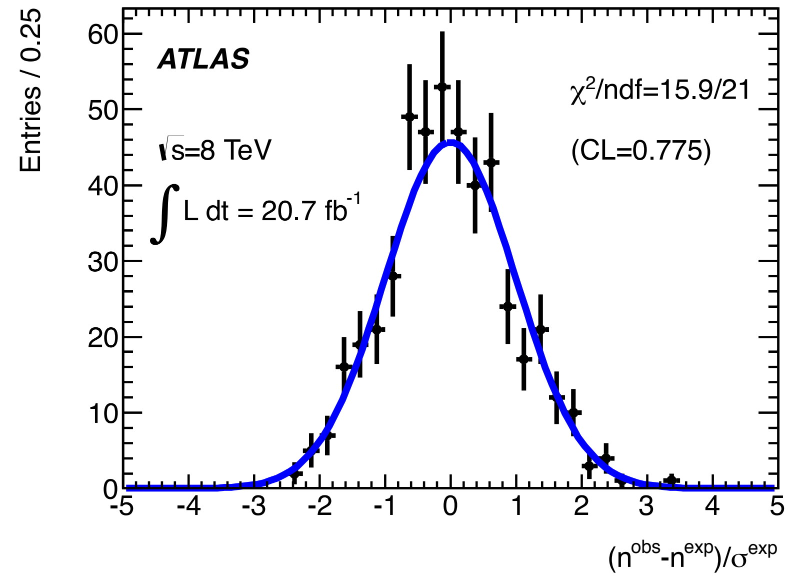

2D analysis assumes no correlation between the two observables. This assumption can be checked in data

Compare the 1D x 1D expectation to the observed events

Gaussian distribution of fluctuations from the $m_{\gamma\gamma}\times\cos(\theta^*)$ expectation → correlations between variables are small

$WW^{(*)}$ channel: signal and background expectations

Process	Expected or observed events
WW	2190 ± 20
WZ/ZZ/Wy	230 ± 10
tt	180 ± 10
tW/tb/tqb	120 ± 10
Z+jets	290 ± 20
W+jets	280 ± 10
Total Background	**3280 ± 20**
Signal J^P=0$^+$	**170 ± 1**
Signal J^P=2$^+$	**110 ± 1**
Observed	**3615**

$WW^{(*)}$ channel: templates in discriminating variables

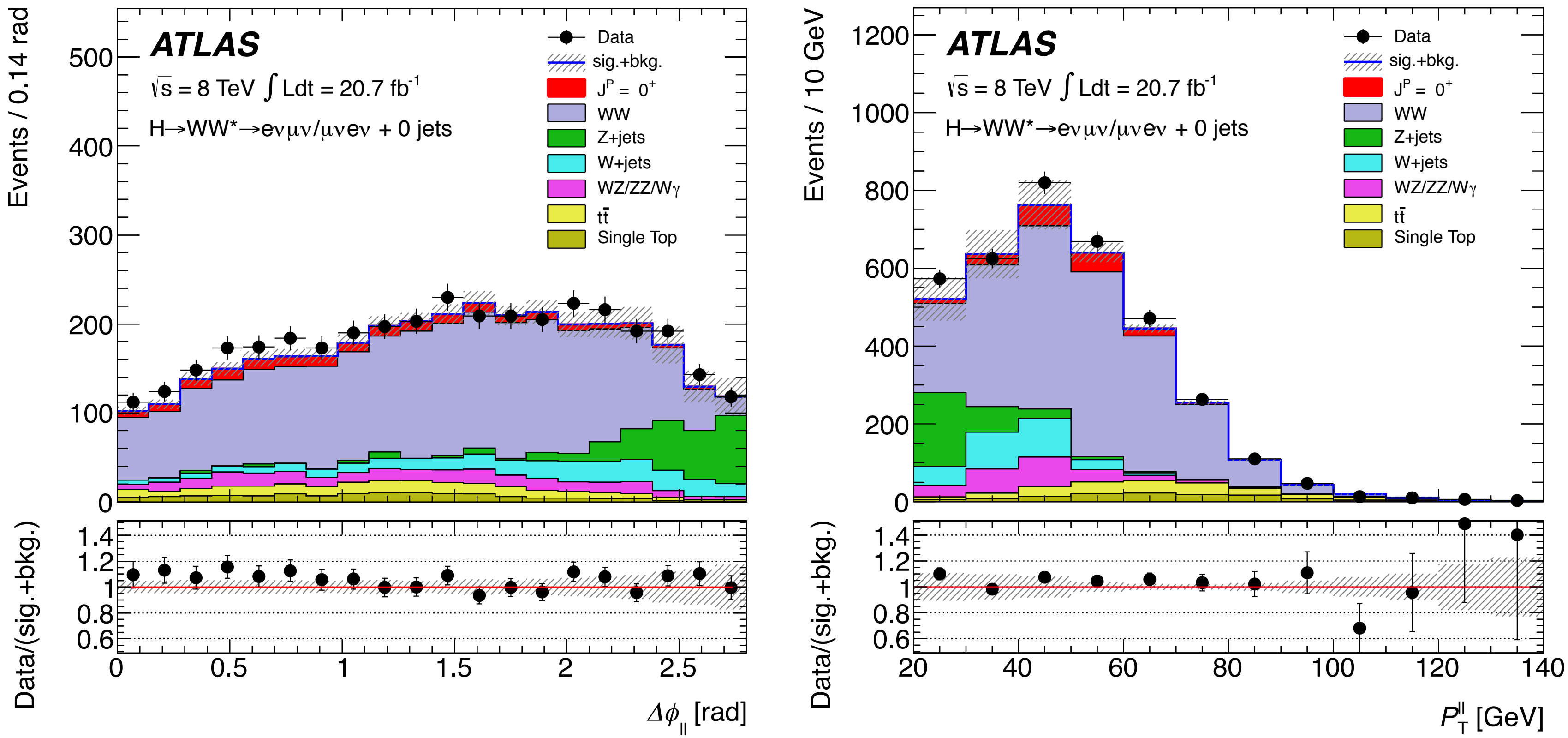

$WW^{(*)}$ channel: templates in discriminating variables

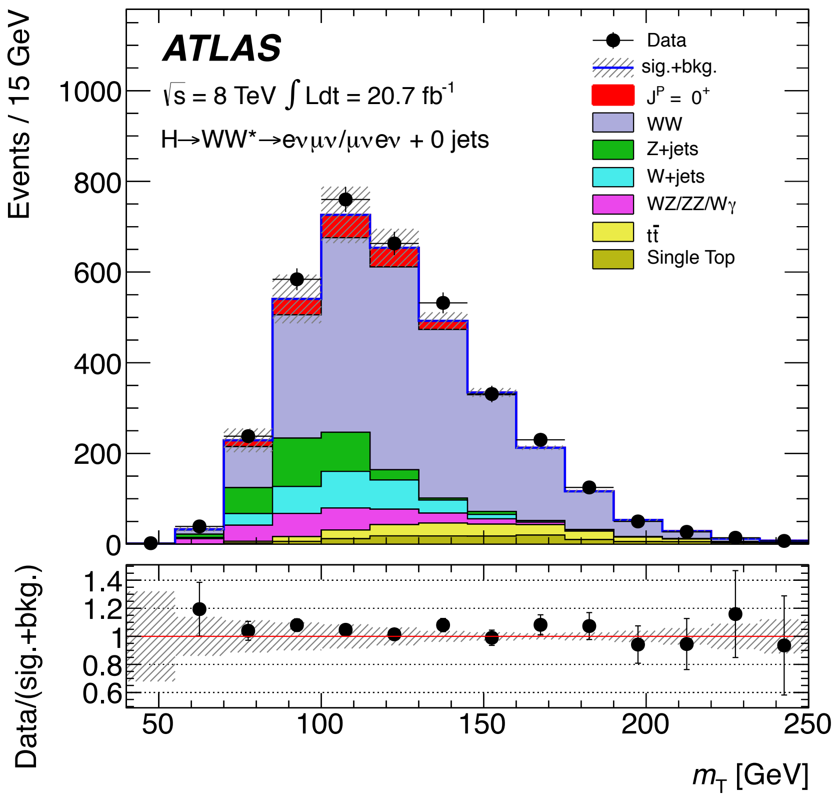

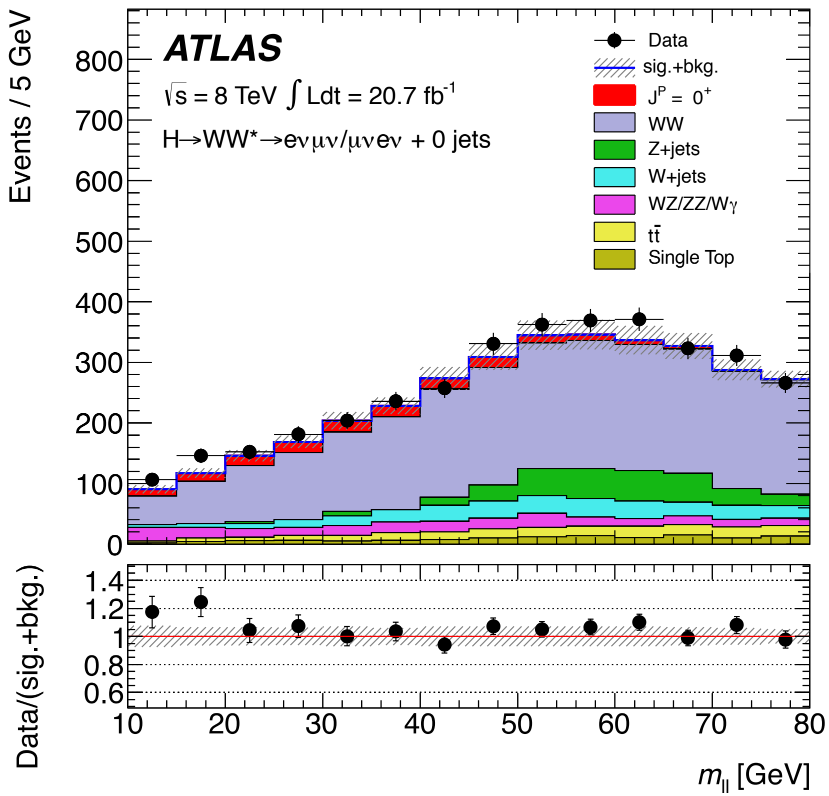

$WW^{(*)}$ channel: systematic uncertainties

Source	Uncertainty (%)
Jet energy scale & resolution	± 9
WW normalisation, theory	± 9
W+jets fake factor	± 8
Lepton scale & resolution	± 6
Other backgrounds, theory	± 5
Pileup modelling	± 4
PDF model	± 4
$E_{\mathrm{T}}^{\mathrm{miss}}$ scale & resolution	± 3

$ZZ^{(*)}$ channel Z+jets control region

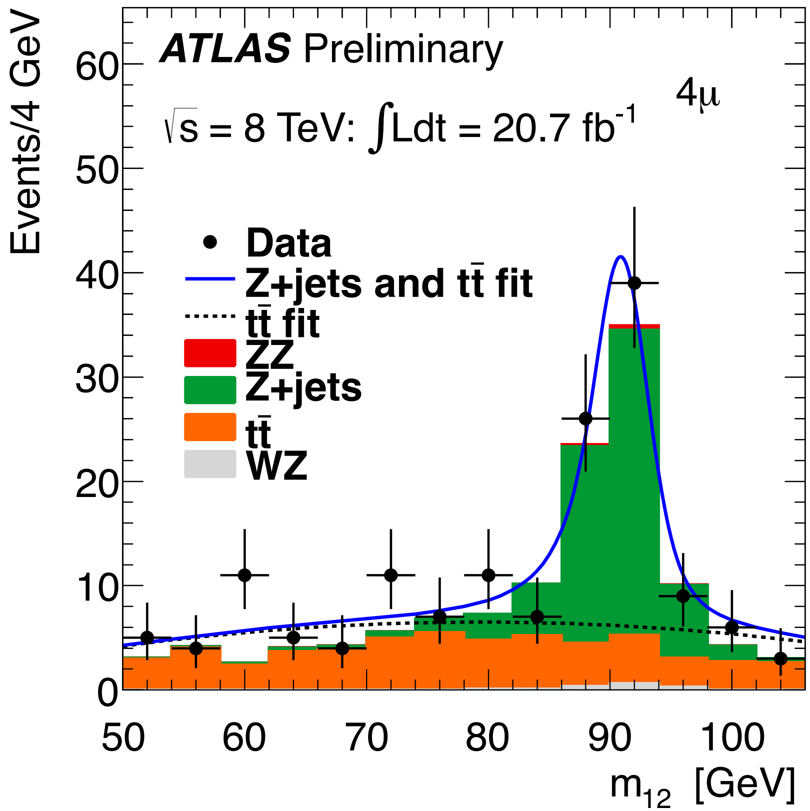

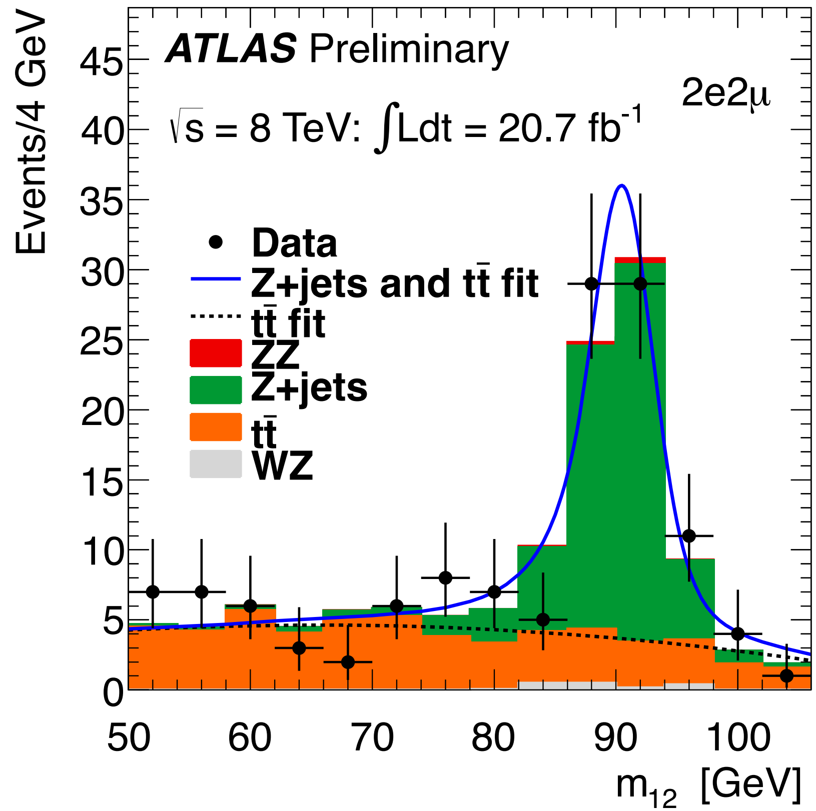

$ZZ^{(*)}$ channel control regions

$ll + \mu\mu$

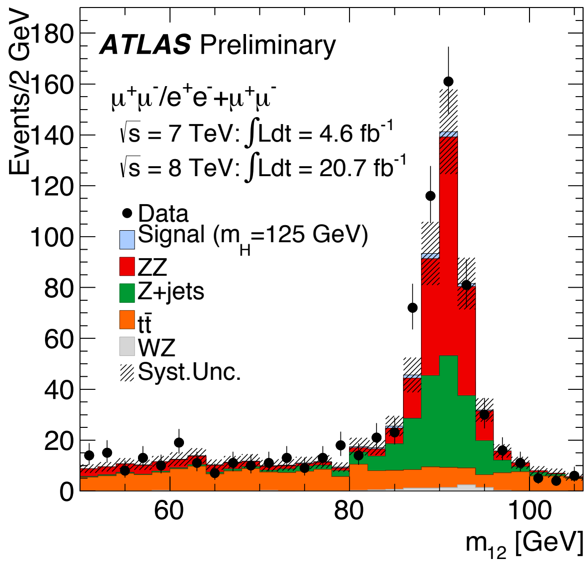

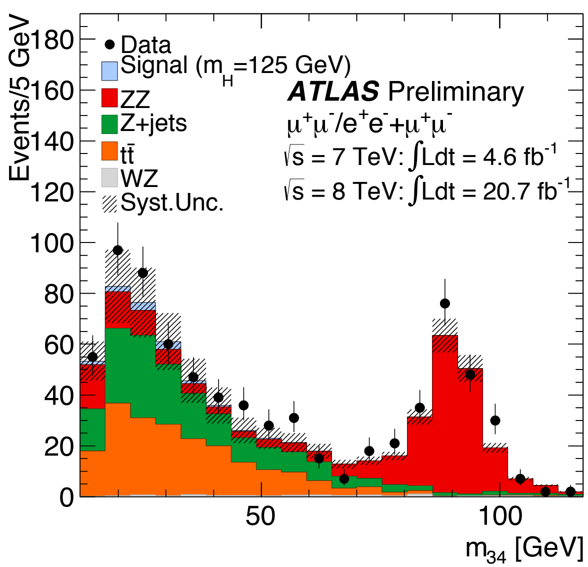

$ll + ee$

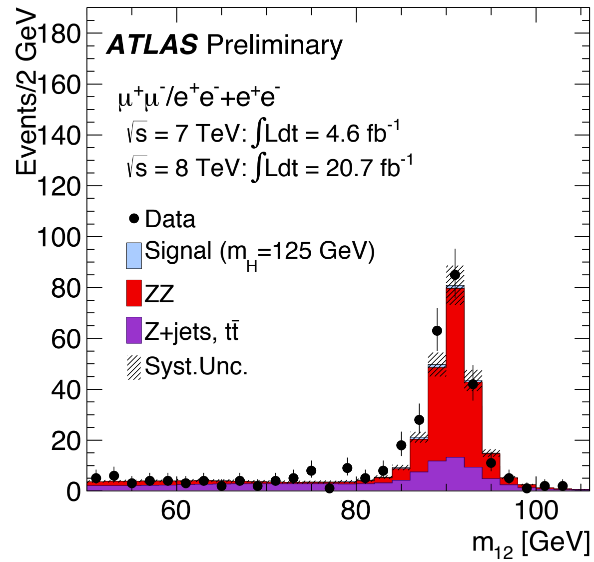

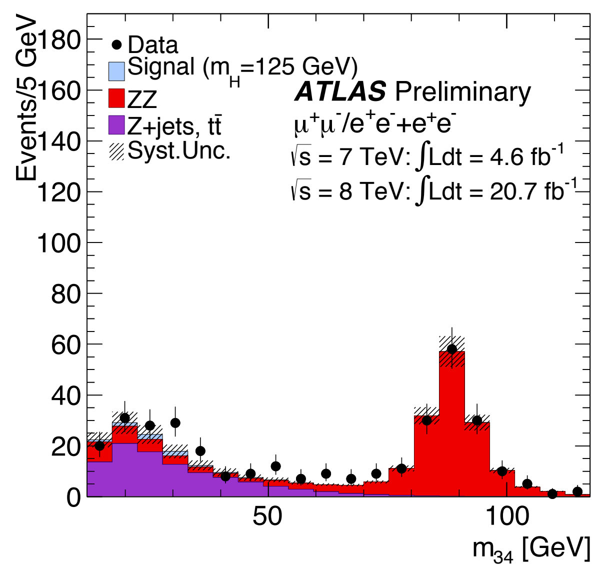

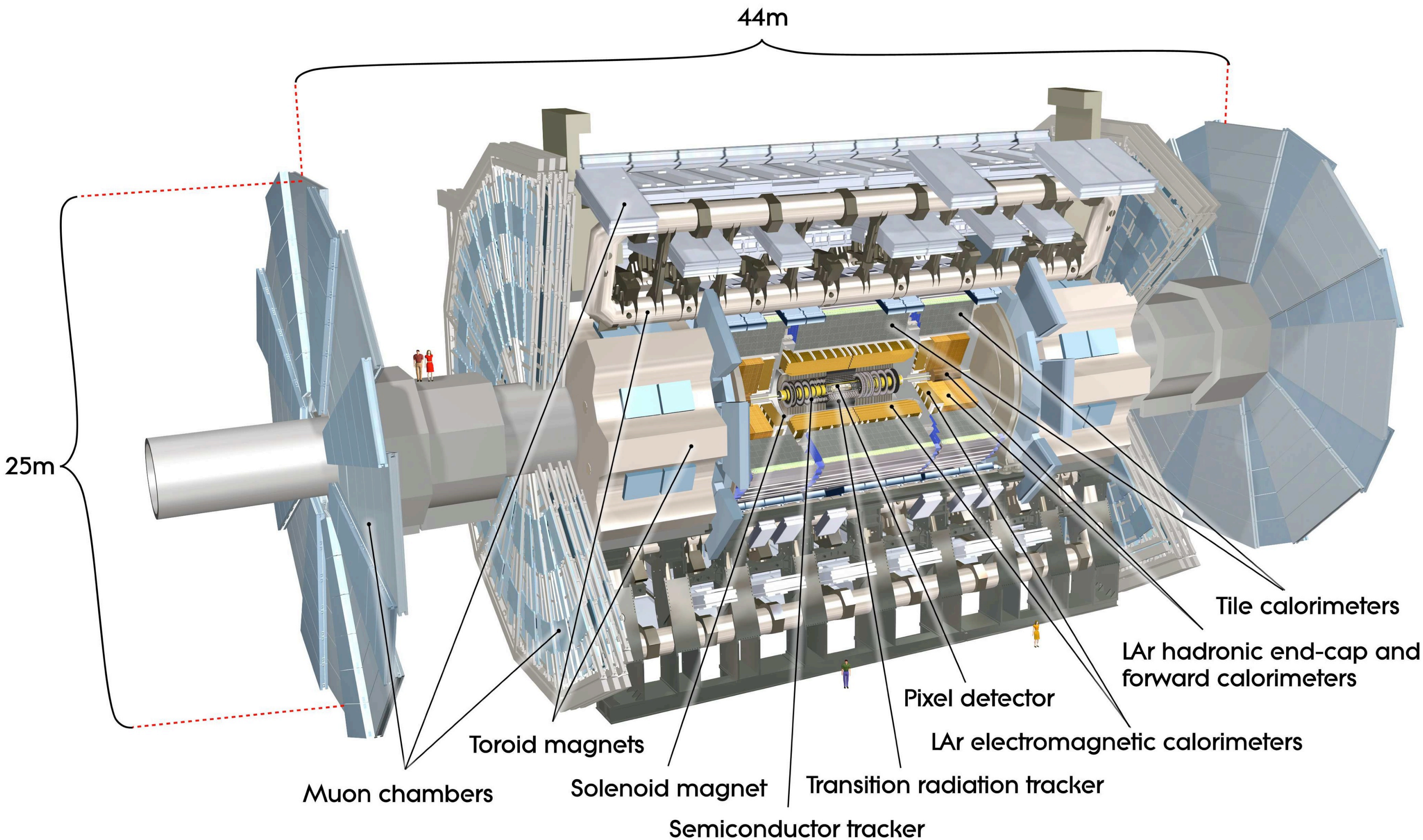
44m
25m
Tile calorimeters
LAr hadronic end-cap and
forward calorimeters
Pixel detector
LAr electromagnetic calorimeters
Toroid magnets
Muon chambers
Solenoid magnet
Transition radiation tracker
Semiconductor tracker

Particle detection with ATLAS